AD-A117 110 NAVAL RESEARCH LAB WASHINGTON DC F/G 12/1
VARIATIONAL ANALYSIS AND APPROXIMATE SOLUTIONS FOR TRANSPORT PH--ETC(U)
JUN 82 G A KERAMIDAS
UNCLASSIFIED NRL-MR-4852 NL

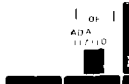

END
DATE FILMED
08-82
DTIC

NRL Memorandum Report 4864

[redacted]

[redacted]

[redacted]

June 30, 1982

SECURITY CLASSIFICATION OF THIS PAGE (When Data Entered)

REPORT DOCUMENTATION PAGE	READ INSTRUCTIONS BEFORE COMPLETING FORM
1. REPORT NUMBER NRL Memorandum Report 4852 2. GOVT ACCESSION NO. AD-A117110	3. RECIPIENT'S CATALOG NUMBER
4. TITLE (and Subtitle) VARIATIONAL ANALYSIS AND APPROXIMATE SOLUTIONS FOR TRANSPORT PHENOMENA	5. TYPE OF REPORT & PERIOD COVERED Interim report
	6. PERFORMING ORG. REPORT NUMBER
7. AUTHOR(s) George A. Keramidas	8. CONTRACT OR GRANT NUMBER(s)
9. PERFORMING ORGANIZATION NAME AND ADDRESS Naval Research Laboratory Washington, DC 20375	10. PROGRAM ELEMENT, PROJECT, TASK AREA & WORK UNIT NUMBERS 61153N23, RR0230141 147002
11. CONTROLLING OFFICE NAME AND ADDRESS Office of Naval Research Arlington, VA 22217	12. REPORT DATE June 30, 1982
	13. NUMBER OF PAGES 82
14. MONITORING AGENCY NAME & ADDRESS(if different from Controlling Office)	15. SECURITY CLASS. (of this report) UNCLASSIFIED
	15a. DECLASSIFICATION/DOWNGRADING SCHEDULE

16. DISTRIBUTION STATEMENT (of this Report)

Approved for public release; distribution unlimited

17. DISTRIBUTION STATEMENT (of the abstract entered in Block 20, if different from Report)

18. SUPPLEMENTARY NOTES

19. KEY WORDS (Continue on reverse side if necessary and identify by block number)

Variational formulation
Approximate solutions
Finite element methods
Transport equation
Convection-diffusion

20. ABSTRACT (Continue on reverse side if necessary and identify by block number)

Certain concepts of classical mechanics are utilized to derive the variational formulation for a field partial differential equation. By introducing suitable parameters, it is demonstrated that the concepts of virtual work and generalized coordinates can be extended to the general transport equation and this equation can be translated into Lagrange's equations of mechanics. The system of equations may represent a large number of physical processes and it is not restricted by any means to a particular problem. The Lagrangian system of equations is most suitable for deriving approximate solutions and this is demonstrated by assuming a linear series expansion in terms of the
(Continued)

DD FORM 1 JAN 73 1473 EDITION OF 1 NOV 65 IS OBSOLETE
S/N 0102-014-6601

SECURITY CLASSIFICATION OF THIS PAGE (When Data Entered)

20. ABSTRACT *(Continued)*

generalized coordinates. Furthermore, it is shown that approximate methods, such as the finite element method, can be directly derived as a special application of the generalized approach. Examples of approximate solutions are given for some typical problems encountered in transport processes.

CONTENTS

A

VARIATIONAL ANALYSIS AND APPROXIMATE SOLUTIONS FOR TRANSPORT PHENOMENA

INTRODUCTION

Approximate methods have been applied to the solution of partial differential equations when analytical forms of solution are not possible due to the nature of the particular problems under study. Some types of approximate solutions can be directly applied to the given equation and some require first the derivation of a variational form of this equation. The latter imposes certain restrictions on applying approximate methods since many of the variational derivations are problem dependent.

The intent of this study is to provide the formulation of a unified analysis for partial differential equations, such as the general transport equation, by methods analogous to those of classical mechanics. The implementation of certain concepts of classical mechanics opens the way to a formulation of the transport equation by means of generalized coordinates and leads to Lagrangian type of equations. This approach simplifies the application of approximate methods for obtaining solutions to many practical problems of interest.

The variational analysis presented here involves a generalization of the concept of virtual work from classical mechanics. The approach was first adapted by M.A. Biot and was applied to heat transfer phenomena and irreversible processes [1,2]. By extending the concept of virtual work to the general transport equation a variational form of this equation can be obtained, which is problem independent, and the resulting variational equation contains terms similar to those found in Lagrangian mechanics. This approach should not be regarded as a "new method" for deriving variational formulations. It is only an application of classical concepts and an extension of Lagrangian mechanics to derive a unified formulation for the transport equation. One of the advantages of such approach is that the physical significance of each term of the differential equation can be easily identified.

Manuscript submitted May 11, 1982.

The governing equation for transport phenomena and the introduction of a vector defined as transport displacement are given in the first section of this study. Based on the definition of the displacement vector the transport equation is written in a form similar to the equation of motion in mechanics. In this form the governing equation will be used in the next section to derive the variational formulation for the transport equation.

According to concepts of classical mechanics two types of variational formulations can be derived, the fundamental form based on variations of the displacement field and the complementary form based on variations of the stress field. The basic definitions and derivations for the variational analysis are given in the second section and the two types of variational formulations are presented for the transport equation. The analogy between the derived equations and those of mechanics can be justified by identifying each of the terms of the variational equations to be similar to such quantities as potential function, dissipation function and generalized body and boundary forces. The dissipation function is a generalization of the concept introduced by Rayleigh in mechanics for systems with viscous dissipation. The resulting Lagrangian equations, in terms of generalized coordinates, represented either type of variational formulation and they are not problem dependent. As a consequence the generalized equations can be used for obtaining solutions to physical problems governed by such equations as the transport equation. Furthermore, many types of approximate solutions can be derived by expressing the field parameters in terms of the generalized coordinates.

A particular example is given in the third section where a series expansion is assumed for the field parameters. This expansion expresses the field parameters as a linear combination of the generalized coordinates. Although such an approximation is restricted by the linear dependence on the generalized coordinates, it may represent such approximations as a Fourier series expansion or an expansion in terms of orthogonal functions. The derivation of the equations in terms of the above approximation is given and it is shown that the finite element methods can be derived as a special case of this approximation [3]. The discretized system of equations for a linear finite element approximation is given as an example and four types of finite element models are derived. Two of the models correspond to the fundamental variational formulation and the other two correspond to the complementary one.

Numerical experiments and solutions to particular problems are given in the fourth section of this study. In the first part of the numerical applications the error behavior of the finite element models is investigated for a given problem with known analytical solutions. Furthermore, the convergence of the models is investigated and the criteria for uniform convergence are discussed. In the second part of the numerical applications, examples of numerical solutions are presented for a number of physical problems. From the example presented the efficiency of the computational models is discussed and one can observe that the unified formulation presented here can be extended to a variety of physical problems.

1. BASIC EQUATIONS AND DEFINITIONS

The general form of a partial differential equation describing transport phenomena, such as mass transfer, heat transfer or species concentration is given by

$$\frac{\partial C(x_k,t)}{\partial t} + \frac{\partial}{\partial x_i}\left[V_i(x_k,t)C(x_k,t)\right] = \frac{\partial}{\partial x_i}\left(k_{ij}\frac{\partial C(x_k,t)}{\partial x_j}\right) + S - K(C - C_o) \tag{1}$$

where C is the transport variable, x_i is the coordinate system, t is the time, V_i is the transport velocity in x_i direction, k_{ij} is the tensor dispersion coefficient, S is the generalized source term and K is the generalized transfer coefficient.

In order to describe the kinematics of a medium, reference is made to two configurations. The reference or initial configuration at time $t = t_o$ and the present configuration at time t with C_o and C the values of the transport variable respectively. A dimensionless transport variable can be defined in terms of C and C_o if one considers the ratio of the change ΔC of the absolute value of the transport variable from the reference to the present state over the absolute value of that variable at the reference state

$$\Theta(x_k,t) = \frac{C - C_o}{C_o} = \frac{\Delta C}{C_o}. \tag{2}$$

In terms of the dimensionless variable Θ, Eq. (1) is expressed as

$$\frac{\partial \Theta}{\partial t} + \frac{\partial}{\partial x_i}(V_i\Theta) = \frac{\partial}{\partial x_i}\left(k_{ij}\frac{\partial \Theta}{\partial x_j}\right) - K\Theta + \frac{1}{C_o}S. \tag{3}$$

From the physical point of view the dimensionless variable Θ can be interpreted as a generalized deformation similar to mechanical strain. Define now a vector field $H_i\ (x_k,t)$ as the *transport displacement vector*, which is a function of the coordinates x_k and time t, of the form

$$\dot{H}_i(x_k,t) = \frac{\partial H_i(x_k,t)}{\partial t} \tag{4}$$

and

$$\Theta(x_k,t) = \frac{\partial H_i(x_k,t)}{\partial x_i} \tag{5}$$

The interpretation of Θ as a deformation or dilatation (strain) is justified by Eq. (5). Furthermore, Eq. (5) may be considered as a constraint in the sense of classical mechanics and it must be verified by the physical solution and by the variations of δH_i and $\delta\Theta$ as

$$\delta\Theta = \frac{\partial}{\partial x_i}\ (\delta H_i). \tag{6}$$

The variations δH_i correspond to virtual displacements with Θ and H_i being analogous to strain and displacement in mechanics. Another quantity, which is defined in mechanics and it is related to deformation, is the stress tensor. Here a similar stress can be defined as

$$\sigma = E\Theta \tag{7}$$

where E is a modulus similar to the bulk modulus in mechanics. Eq. (7) may represent a constitutive relation for a particular medium and together with Eq. (3) describes the behavior of that medium under certain loading conditions.

The governing equation can be expressed in terms of the displacement field as

$$\frac{\partial H_i}{\partial t} + V_i\Theta = k_{ij}\ \frac{\partial\Theta}{\partial x_j} - KH_i + \dot{h}_i \tag{8}$$

where h_i satisfied the equation

$$\frac{\partial h_i}{\partial x_i} = \frac{1}{C_o}\int_0^t S dt. \tag{9}$$

This equation does not uniquely determine h_i but any particular field may be chosen to satisfy Eq. (9). Such a field may be considered to be a given function of the coordinates and time. The dispersion coefficient is a tensor with six components and with the property

$$k_{ij} = k_{ji},$$

hence, k_{ij} is a symmetric tensor. If λ_{ij} is the inverse of k_{ij} then λ_{ij} is also symmetric and Eq. (8) can be written as

$$\lambda_{ij}\left(\frac{\partial H_i}{\partial t} + V_i\Theta\right) + \lambda_{ij}(KH_i - \dot{h}_i) = \frac{\partial \Theta}{\partial x_j} \tag{10}$$

Equations (5) and (8) represent a formulation which is defined as the displacement formulation for the transport equation and this formulation reduces to the conventional one, Eq. (3), by combining Eqs. (5) and (8). Furthermore, the three equations, Eqs. (5), (7) and (8), are analogous to the kinematic relations, stress-strain relations and the momentum equation in mechanics.

The concept of transport displacement has been introduced previously by the author, under the name of heat displacement, for describing heat transfer processes [4]. In general, transport processes can be described either by the conventional transport equation, Eq. (3), or by the two equivalent equations, Eqs. (5) and (8). The introduced transport displacement is regarded as a generalized quantity conjugate to the generalized deformation Θ. This generalized presentation of the governing equation for transport phenomena has certain features which will be discussed in the next sections.

2. VARIATIONAL ANALYSIS

A large number of variational formulations have been introduced in the past for deriving approximate solutions. The majority of them are based on the minimization of a functional which describes a particular physical process. Such formulations are usually restricted to the conditions of the particular problem and their applicability is limited. One wishes to have a unified approach for deriving variational formulations. Such formulations should be problem independent and they should be derived from physical considerations.

Classical mechanics has provided researchers with some powerful tools for solving problems either analytically or by approximate methods. One such a tool is the principle of virtual work which has been successful in solving a variety of problems. The principle of virtual work in mechanics has been extended to such areas as thermodynamics [5] and variational equations can be derived which are not

problem dependent for a variety of physical processes. Another concept largely used in mechanics is the concept of generalized coordinates which can be used to describe a physical system. Generalized coordinates can be interpreted as generalized displacements or velocities which specify the configurations of a physical system [6].

The application of these concepts are not restricted to mechanics or only to certain media. In this section the concept of virtual work is used to derive two variational formulations for the transport equation. The first is referred to as the fundamental form and is based on the displacement formulation of the transport equation. The second formulation is based on the conventional form of the transport equation and is referred to as the complementary form. These two forms are directly analogous to the ones in classical mechanics where the fundamental form of a variational principle is given in terms of variations of the displacement field and the complementary form in terms of forces. Both of these forms are based on equilibrium or conservation laws governing the physical system.

2.1 Fundamental Variational Principle

The fundamental form is derived from the displacement formulation of the transport equation by implementing the principle of virtual work. Consider a variation δH_i of the displacement field H_i and the corresponding variation $\delta\Theta$ given by the constraint Eq. (6). If the medium is subjected to a virtual displacement δH_i, then the principle of virtual work requires that

$$\int_v \left[\lambda_{ij}\left(\frac{\partial H_i}{\partial t} + V_i\Theta\right) + \lambda_{ij}(KH_i - \dot{h}_i) - \frac{\partial\Theta}{\partial x_j}\right]\delta H_j \, dv = 0, \tag{11}$$

where the integration is extended over a volume v of the medium. Integration of Eq. (11) by parts yields

$$\int_v \lambda_{ij}\left(\frac{\partial H_j}{\partial t} + V_i\Theta\right)\delta H_i dv + \int_v \Theta \frac{\partial}{\partial x_i}(\delta H_i) dv + \int_v \lambda_{ij}(KH_j - \dot{h}_j)\delta H_i dv = \int_s \Theta n_i \delta H_i ds. \tag{12}$$

The surface integral is extended over the boundary surface s of the control volume v and n_i is the unit vector normal to the boundary pointing outward. The second term of the left hand side is written as

$$\int_v \Theta\delta\left[\frac{\partial H_i}{\partial x_i}\right]dv = \int_v \Theta\delta\Theta\, dv = \delta P \tag{13}$$

and the scalar function P may be interpreted as a potential function, similar to the potential function of mechanics, given by

$$P = 1/2 \int_v \Theta^2 dv. \tag{14}$$

In terms of the variations δP, Eq. (12) is written as

$$\int_v \lambda_{ij}\left[\frac{\partial H_j}{\partial t} + V_j\Theta\right]\delta H_i dv + \int_v \lambda_{ij}(KH_j - \dot{h}_j)\,\delta H_i dv + \delta P = \int_s \Theta n_i \delta H_i\, ds. \tag{15}$$

The variational relation given by Eq. (15) can be considered as the variational principle for the transport equation. Equation (15) must be verified for arbitrary variations of the displacement field H_i, with Θ defined as a function of H_i through the constraint, Eq. (5). Hence the variational equation given by Eq. (15) is nothing but a variational statement for the transport equation with energy conservation automatically satisfied. This variational principle must be understood in a broad sense since it corresponds to the principle of virtual work in mechanics. It represents the fundamental form since it was derived in terms of the displacement field.

2.2 Complementary Variational Principle

In the preceding section the fundamental form of the variational principle was derived for the transport equation. The analogy with mechanics suggests that it is possible to derive a complementary form of the variational principle for the same equation. Since the generalized deformation Θ, Eq. (5), leads to the definition of the generalized stress σ, which is similar to the mechanical stress, then the complementary form is derived by varying the stress field and expressing the conservation equation, Eq. (3), in variational form.

In terms of the generalized stress σ, Eq. (3) is written as

$$\frac{\partial\sigma}{\partial t} + \frac{\partial}{\partial x_i}(V_i\sigma) - \frac{\partial}{\partial x_i}\left[k_{ij}\frac{\partial\sigma}{\partial x_j}\right] + K\sigma - \frac{1}{C_o E}S = 0 \tag{16}$$

and for arbitrary variation $\delta\sigma$ an equivalent to Eq. (11) is obtained as

$$\int_v \left[\frac{\partial\sigma}{\partial t} + \frac{\partial\sigma}{\partial x_i}(V_i\sigma) - \frac{\partial}{\partial x_i}\left[k_{ij}\frac{\partial\sigma}{\partial x_j}\right] + K\sigma - \frac{1}{C_o E}S\right]\delta\sigma\, dv = 0. \tag{17}$$

Integration by parts yields

$$\int_v \left[\frac{\partial \sigma}{\partial t} + \frac{\partial}{\partial x_i}(V_i \sigma)\right] \delta\sigma \, dv + \int_v k_{ij} \frac{\partial \sigma}{\partial x_j} \frac{\partial}{\partial x_i}(\delta\sigma) \, dv + \int_v \left[K\sigma\delta\sigma - \frac{1}{C_o E} S\delta\sigma\right] dv = \int_s k_{ij} n_j \frac{\partial \sigma}{\partial x_j} \, ds. \tag{18}$$

The surface integral is extended to the boundary surface s of the volume v and n_i denotes the unit vector normal to the boundary pointing outwards. Proceeding as in the previous section Eq. (18) is written as

$$\int_v \left[\frac{\partial \sigma}{\partial t} + V_i \frac{\partial \sigma}{\partial x_i}\right] \delta\sigma \, dv + \int_v \left[K\sigma - \frac{1}{C_o E} S\right] \delta\sigma \, dv + \delta P = \int_s n_i k_{ij} \frac{\partial \sigma}{\partial x_j} \delta\sigma \, ds \tag{19}$$

where the variation δP is given by

$$\delta P = \int_v \left[k_{ij} \frac{\partial \sigma}{\partial x_j} \delta\left(\frac{\partial \sigma}{\partial x_i}\right) + \frac{\partial V_i}{\partial x_i} \sigma\delta\sigma\right] dv \tag{20}$$

and the scalar P by

$$P = 1/2 \int_v \left[k_{ij} \frac{\partial \sigma}{\partial x_j} \frac{\partial \sigma}{\partial x_i} + \frac{\partial V_i}{\partial x_i} \sigma^2\right] dv. \tag{21}$$

Equation (19) represents the complementary form of the variational principle for the transport equation. The different terms of the variational equation, Eq. (19) may be evaluated either in terms of the generalized stress σ or in terms of the deformations Θ. The latter case corresponds to formulating the variational principle for the transport equation in terms of a primitive dimensionless variable Θ.

The two forms of variational principles derived previously are generalized statements of conservation laws for a physical system and their existence is verified by concepts from classical mechanics. Either form can be applied to the governing equation of many physical processes, but it first is necessary to derive a more compact form of these variational equations which will be better suited to practical applications. Some remarks can be made regarding the form of the variational equations. A significant difference between the two forms is the fact that the complementary form involves space derivatives of the transport variable Θ. This does not present a problem as long as the space distribution for Θ is continuous. If discontinuities exist, as is the case in many practical problems, then the complementary form is not the appropriate one to be used for the solution of such a problem. In gen-

eral, when using the same approximate representation for the transport variable Θ, the complementary principle will yield results which are less accurate than those obtained by the fundamental form which is based on the displacement field.

2.3 Generalized Coordinates

A physical system is usually described by a set of coordinates and the governing equations are expressed in terms of these coordinates. In many cases, a given set of coordinates is not the most convenient one to describe a physical problem. As an example, for certain problems involving the motion of a particle it is more convenient to use a moving coordinate system than a fixed one. It would be very desirable, and practical, to have a general method for describing a physical system by a set of coordinates which will provide a uniform method to represent and solve the governing equations for physical processes. Such a set is given by the generalized coordinates of classical mechanics. A set of generalized coordinates is any set of coordinates by means of which the position of a particle in a system may be specified. The concept of the generalized coordinates and the method for describing a physical system in terms of these coordinates was first introduced by Lagrange.

When a physical system is described by a set of generalized coordinates, it is the usual practice to designate each coordinate by q and the set of n generalized coordinates by q_k, $k = 1, \ldots, n$. For a physical system of N particles a set of $3N$ generalized coordinates may be specified, and since these coordinates must have some definite set of values they will be functions of the time and also of the cartesian system of coordinates. For a physical system which is described by a set of generalized coordinates q_k, the time derivative $\dot{q}_k$ is defined as a generalized velocity associated with this coordinate. This generalized velocity, for example, can be computed in terms of cartesian coordinates and velocities. If one assumes that q_k is a function of the cartesian coordinates x_i and time t, then

$$q_k = q_k(x_i, t)$$

It is also possible to express the cartesian coordinates in terms of generalized coordinates as

$$x_i = x_i(q_k, t)$$

From the definition of the generalized velocity one obtains

$$\dot{x}_i = \frac{\partial x_i}{\partial t} + \frac{\partial x_i}{\partial q_k}\,\dot{q}_k$$

Other physical quantities, such as energy, momentum, forces etc. can be expressed in terms of the generalized coordinates. For example the generalized momentum p_k associated with the coordinate q_k is given by

$$p_k = \frac{\partial T}{\partial \dot{q}_k}$$

when T is the kinetic energy in terms of q_k.

The subject of this section is to implement the concept of generalized coordinates to the two forms of variational equations previously derived. By introducing generalized coordinates into the variational equations, they can be translated into a Lagrangian type of equations. This provides a unified approach and the transport equation is represented in a generalized form independent of coordinate systems or physical conditions.

Consider the displacement field H_i to be a function of a set of n generalized coordinates q_k,

$$H_i = H_i\,(q_k,\, x_j,\, t). \tag{22}$$

The variations of H_i, or small displacements δH_i, are due entirely to the variations of the generalized coordinates δq_k and they are expressed as

$$\delta H_i = \frac{\partial H_i}{\partial q_k}\,\delta q_k. \tag{23}$$

The variations δq_k can be identified as virtual displacements since they do not necessarily represent any actual motion but only any possible motion of a system. Under such a motion there is an amount of work done which is defined as the virtual work δW and it is expressed as

$$\delta W = Q_k\,\delta q_k \tag{24}$$

where Q_k is defined as a generalized force associated with the coordinate q_k.

The variations of the potential function P, given by Eq. (14), are expressed as

$$\delta P = \frac{\partial P}{\partial q_k}\,\delta q_k \tag{25}$$

and the time derivative of the displacement vector is taken as

$$\dot{H}_i = \frac{\partial H_i}{\partial q_k}\,\dot{q}_k + \frac{\partial H_i}{\partial t} \tag{26}$$

Equation (26) expresses the total time derivative of the vector H_i and by differentiating with respect to the generalized velocity $\dot{q}_k$ one obtains

$$\frac{\partial \dot{H}_i}{\partial \dot{q}_k} = \frac{\partial H_i}{\partial q_k} \tag{27}$$

Taking into account Eqs. (23), (25), (26) and (27), the variational principle, Eq. (15), can be transformed into a more compact form. The first term of Eq. (15) is written as

$$\int_v \lambda_{ij}\left[\frac{\partial H_i}{\partial t} + V_i\Theta\right]\delta H_j\,dv = \int \lambda_{ij}\left[\frac{\partial H_i}{\partial t} + V_i\Theta\right]\frac{\partial \dot{H}_j}{\partial \dot{q}_k}\,\delta q_k\,dv = \frac{\partial D}{\partial \dot{q}_k}\,\delta q_k \tag{28}$$

where the function D is given by

$$D = 1/2\int_v \lambda_{ij}(\dot{H}_i + V_i\Theta)(\dot{H}_j + V_j\Theta)\,dv = 1/2\int_v \lambda_{ij}\dot{H}_i^{\bullet}\dot{H}_j^{\bullet}\,dv \tag{29}$$

and the vector $\dot{H}_i^{\bullet}$ is given by

$$\dot{H}_i^{\bullet} = \dot{H}_i + V_i\Theta. \tag{30}$$

The vector $\dot{H}_i^{\bullet}$ can be regarded as the total rate of the transport displacement and the function D defines a dissipation function. A physical interpretation of both of these qualities can be given if one considers some particular case of a physical process. For example, if the transport equation describes heat transfer, then the vector $\dot{H}_i^{\bullet}$ represents the total convective and diffusive local rate of heat flow and the function D the total dissipation of the physical process. This dissipation has been previously introduced for systems with friction or viscous effects and it is known as Rayleigh's dissipation function.

In terms of the variations δP and δD, Eq. (15) yields

$$\delta D + \delta P = \int_s \Theta\eta_i\,\frac{\partial H_i}{\partial q_k}\,\delta q_k\,ds + \delta F. \tag{31}$$

The term δF of the right hand side of Eq. (31) combines the source and transfer terms and is given by

$$\delta F = \int_v \lambda_{ij}(-KH_j + \dot{h}_j)\,\frac{\partial H_i}{\partial q_k}\,\delta q_k\,dv. \tag{32}$$

and

$$F = \int_v \lambda_{ij} \left[-\frac{K}{2} H_i H_j + \dot{h}_j H_i \right] dv \tag{33}$$

The surface integral of the right hand side of Eq. (31) can be expressed in terms of a generalized boundary force Q_k as

$$\int_s \Theta \eta_i \frac{\partial H_i}{\partial q_k} \delta q_k \, ds = Q_k \delta q_k \tag{34}$$

where

$$Q_k = \int_s \Theta \eta_i \frac{\partial H_i}{\partial q_k} \, ds. \tag{35}$$

From the physical point of view, Eq. (34), can be interpreted as the virtual work, δW, done by the force Q_i on the inflow of a volume of fluid per unit area associated with the virtual displacement δq_k Comparing Eqs. (24), (31) and (34) the relation

$$\delta D + \delta P - \delta F = \delta W \tag{36}$$

is obtained. This can be regarded as expressing conservation since the virtual work done by the generalized boundary forces is equal to energy gain or loss for a physical system.

For arbitrary variations of the generalized coordinates Eq. (36) is written as

$$\frac{\partial D}{\partial \dot{q}_k} + \frac{\partial P}{\partial q_k} = Q_k + \frac{\partial F}{\partial q_k}. \tag{37}$$

For the set of n generalized coordinates Eqs. (37) constitute a system of n differential equation for the unknowns q_k. These equations are of the same form as the equations of Lagrangian mechanics for the slow motion of a dissipative system with negligible inertia forces. For example, for the particular case of heat transfer the potential function is regarded as a thermal potential and the function D as the total heat dissipation function. The function F may be due to internal heat generation and/or heat transfer. Furthermore, the generalized forces Q_k represent thermal forces due to the temperature distribution at the boundary and they are defined by Eq. (34) as the work done by Q_i under the displacement δq_k.

This generalized derivation in terms of the generalized coordinates, can be extended to the complementary form of the variational principle. The derivation is identical and it yields a set of equations

similar to Eqs. (37), the difference being that they are derived in terms of the transport variable Θ. If one assumes that Θ is a function of a set of n generalized coordinates $\bar{q}_k$, then

$$\Theta = \Theta(\bar{q}_k, x_i, t). \tag{38}$$

Following the same steps as for the previous derivations the Lagrangian equations are

$$\frac{\partial \bar{D}}{\partial \dot{\bar{q}}} + \frac{\partial \bar{P}}{\partial \bar{q}_k} = \bar{Q}_k + \frac{\partial \bar{F}}{\partial \bar{q}_k} \tag{39}$$

where

$$\bar{D} = 1/2 \int_v \left[\dot{\Theta} + V_i \frac{\partial \Theta}{\partial x_i}\right]\left[\dot{\Theta} + V_j \frac{\partial \Theta}{\partial x_j}\right] dv \tag{40}$$

$$\bar{P} = 1/2 \int_v \left[k_{ij} \frac{\partial \Theta}{\partial x_i}\frac{\partial \Theta}{\partial x_j} + \frac{\partial V_i}{\partial x_i}\Theta^2\right] dv \tag{41}$$

$$\bar{F} = \int_v \left[-1/2\ K\Theta^2 + \frac{1}{C_o} S\Theta\right] dv \tag{42}$$

and

$$\bar{Q}_k = \int_s k_{ij} \eta_i \frac{\partial \Theta}{\partial x_j}\frac{\partial \Theta}{\partial \bar{q}_k}\, ds. \tag{43}$$

As one may observe from Eqs. (40) to (43) the complementary variational principle translates to similar types of equations as the fundamental form, but there is an important difference between the two formulations. The latter form involves spatial derivatives of the transport variable Θ in the expressions for the functions $\bar{D}$, $\bar{P}$ and the generalized forces $\bar{Q}_i$. This is a disadvantage of the complementary form, as it was mentioned earlier, especially for applications to problems with discontinuities on the distribution of the primitive variables. Although each of the formulations was derived in terms of a different set of coordinates both can be represented by the same type of generalized equations. This is verified by the unified approach used to derive the Lagrangian type of equations and also by the fact that the transport variable Θ and the displacement field are conjugate variables related by the constraint Eq. (5).

The concept of generalized coordinates provides the basis for deriving the Lagrangian formulation of the transport equation. From the physical point of view the generalized coordinates can describe a system completely and the Lagrangian equations can provide an accurate formulation of the physical

problem. A particular advantage of the formulation is that it was derived independently of a particular representation of the field variables. Furthermore, the above analysis can be extended to many physical systems governed by equations other than the transport equation.

The Lagrangian types of equations derived in this section do not represent a new mathematical theory but a different way of expressing a conservation law. The main feature of these equations is the manner in which they were derived. It is evident that these equations have the same form in any system of coordinates and from classical mechanics one can verify that the functions involved in Lagrange's equations have the same value for any coordinate system. The unified form of these equations is of great value not only for advanced formulations in mechanics but they also provide a starting point for approximate solutions to physical problems.

3. APPROXIMATE METHODS

The partial differential equation describing transport phenomena was transformed into a set of ordinary differential equations expressed in terms of generalized coordinates. The equations obtained can be solved analytically for a number of physical problems. For many of the problems encountered in practical applications, analytical solutions are not easy to obtain and approximate or numerical solutions are sought.

The generalized nature of the previously obtained equations is most appropriate for applying approximate solutions. Since these equations are given in terms of generalized coordinates, the field variables describing the physical process are assumed to be functions of these generalized coordinates. Many different expressions or combinations of the generalized coordinates can be used to form the functional representing the field variable. In order to demonstrate the procedure one may assume a linear dependence of the field variables on the generalized coordinates. This specific representation by no means restricts the previously derived formulations to only linear functional approximation. The main reason for such a choice is the fact that a variety of numerical solutions are based in such approximations and as will be shown later the finite element method can be derived as a special case of the generalized formulations.

3.1 Linear Functionals

The linear dependence of the displacement field H_i on the generalized coordinates is expressed as

$$H_i(q_k, x_j, t) = f_{ik}(x_j) q_k(t) \tag{44}$$

The generalized coordinates q_k may be functions of time and they are treated as the coordinates describing the physical system. From the physical point of view they represent degrees of freedom and the functions f_{ik} (x_j) specify the extent to which q_k participate in the functions $H_i(x_j,t)$. The approximation of the displacement field given by Eq. (44) is quite general since no specific expressions are given for the functions f_{ik}. Furthermore, Eq. (44) may represent approximations such as Fourier series or series expansions in terms of orthogonal functions. Similar approximations can be used for the transport variable Θ.

In the following the fundamental form of the variational principle will be used to derive the approximate system of equations for obtaining numerical solutions. For the complementary form the derivation will not be given since it is identical to that of the fundamental form.

The Lagrangian type of equation given by Eq. (37) can be translated to a system of ordinary differential equations in terms of the generalized coordinates q_k by using the approximation, Eq. (44), for the displacement field and by first defining the time and spatial derivatives as

$$\dot{H}_i = \dot{q}_k f_{ki} \tag{45}$$

and

$$\Theta = \frac{\partial H_i}{\partial x_i} = q_k f_{ki,i}. \tag{46}$$

In terms of these definitions the dissipation function D is evaluated as

$$D = 1/2 \int_v \lambda_{ij} (\dot{q}_k f_{ki} + V_i q_k f_{km,m})(\dot{q}_l f_{lj} + V_j q_l f_{ln,n}) dv$$

or

$$D = 1/2\ d_{ij} \dot{q}_i \dot{q}_j + v_{ij} \dot{q}_i q_j$$

where

$$d_{ij} = \int_v \lambda_{kl} f_{ki} f_{lj} dv \tag{47}$$

and

$$v_{ij} = \int_v \lambda_{kl} V_k f_{il} f_{jm,m} dv. \tag{48}$$

Similarly, the potential function P is evaluated as

$$P = 1/2\ p_{ij} q_i q_j \tag{49}$$

where

$$p_{ij} = \int_v f_{ik,k} f_{jl,l} dv. \tag{50}$$

The function F transforms to the form

$$F = S_i q_i - 1/2 w_{ij} q_i q_j$$

where

$$S_i = \int_v \lambda_{ki} \dot{h}_l f_{kl} dv \tag{51}$$

and

$$w_{ij} = \int_v = \int_v K \lambda_{kl} f_{ik} f_{jl} dv. \tag{52}$$

Finally the boundary forces Q_i are expressed as

$$Q_i = \int_s \Theta \eta_j f_{ij} ds \tag{53}$$

Substituting the expressions for D, P, F, and Q_i from the above equations into Eq. (44) yields

$$d_{ij} \dot{q}_j + (v_{ij} + p_{ij} + w_{ij}) q_j = Q_i + S_i. \tag{54}$$

This matrix equation represents a system or ordinary differential equations for the unknown field parameters q_i, which may represent displacements. The generalized coordinates describe the physical system by means of a large but finite number of variables and their number will determine the size of the above system of equations. The solution of Eq. (54) yields the approximate solution for the transport equation. The order of approximation of the numerical solution is determined by the functions $f_{il}(x_k)$ and depends on the accuracy of the solution required and usually on the complexity of the physical problem.

For the evaluation of the matrix coefficients of Eq. (54) the integration domain is considered to be taken over the volume v in the n-space of the coordinates x_i, where

$$dv = dx_1\ dx_2 \ldots dx_n.$$

In a more general sense the integration domain can be extended over all $n + 1$ coordinates x_i and t instead of only the n coordinates x_i, where

$$d\tau = dx_1,\ dx_2 \ldots dx_n\ dt.$$

This extension of the integration domain will yield the same Lagrangian-type equations since the unknown physical quantities can be expressed in any functional form in terms of generalized coordinates. For this particular case the approximation given by Eq. (44) will be replaced by

$$H_i(x_k,t) = f_{ij}(x_k)\, g_n(t)\, q_j^n. \tag{55}$$

It should be noted that the approximation given by Eq. (55) is more restrictive in nature than the one given by Eq. (44) since one assumes a known dependence of the variables on time through the function $g_n(t)$. The generalized coordinates, in this case q_i^n, represent values at the i th point in space and at the n th point in time. The respective time and spatial derivatives of Eq. (55) yield

$$\begin{aligned} \dot{H}_i &= f_{ij}(x_k)\, \dot{g}_n(t)\, q_j^n \\ H_{i,i} &= f_{ij,i}(x_k)\, g_n(t)\, q_j^n. \end{aligned} \tag{56}$$

A system of equations in terms of the generalized coordinates q_i^n can be obtained by substituting the approximation given by Eq. (55) into the Lagrangian equations. The expressions for D, P, F and Q_i are evaluated as for the previous approximations and they are

$$\begin{aligned} D &= 1/2\ [d_{ijkl} + v_{ijkl}]\ q_i^k q_j^l \\ P &= 1/2 p_{ijkl} q_i^k q_j^l \\ F &= S_{ik} q_i^k - 1/2 w_{ijkl} q_i^k q_j^l \end{aligned} \tag{57}$$

where

$$\begin{aligned} d_{ijkl} &= \int_\tau \lambda_{mn} f_{im} f_{jn} \dot{g}_k \dot{g}_l\, d\tau \\ v_{ijkl} &= \int_\tau \lambda_{mn} V_m f_{in} f_{js,s} g_k g_l\, d\tau \\ p_{ijkl} &= \int_\tau f_{im,m} f_{jn,n} g_k g_l\, d\tau \\ S_{ik} &= \int_\tau \lambda_{mn} \dot{h}_n f_{mi} g_k\, d\tau \\ w_{ijkl} &= \int_\tau K \lambda_{mn} f_{im} f_{jn} g_k g_l\, d\tau. \end{aligned} \tag{58}$$

Substituting the above expressions into the Lagrangian Eq. (44) yields

$$[d_{ijkl} + v_{ijkl} + p_{ijkl} + w_{ijkl}] q_i^k = Q_j^l + S_{jl} \qquad \begin{matrix} i,j = 1,n \\ k,l = 1,m \end{matrix} \tag{59}$$

where the boundary forces Q_j^l are given by

$$Q_j^l = \int_s \eta_i f_{km,m} f_{ij} g_l g_k \, ds. \tag{60}$$

The matrix Eq. (59) represents a system of $n + m$ algebraic equations for the unknown field parameters, the generalized coordinates q_l^k, and the domain of integration τ of the matrix coefficients is extended over the $n + 1$ coordinates x_i and t.

The Lagrangian type of equations and the two systems of differential and algebraic equations derived in this section represent two examples of approximate methods which can be applied to solve problems on transport processes. The application of the derived formulation to a physical system can be carried out by dividing the domain of the system into a finite number of subdomains connected by common boundaries. Each of these domains constitutes a sub-system that can be analyzed separately by the system of equations derived in terms of generalized coordinates. For each sub-system s the two systems of equations may be written in a general form as

$$A_{ij}^{(s)} q_j = Q_i^{(s)}, \tag{61}$$

where q_i are the generalized coordinates for the sub-system s, $Q_i^{(s)}$ are the associated generalized boundary forces and $A_{ij}^{(s)}$ the matrix coefficients of the system of equations which were derived from the Lagrangian equation for the domain s. Taking the sum of Eq. (61) over all the domains of the sub-systems, the equation for the total system is written as

$$A_{ij} q_j = Q_i, \tag{62}$$

where A_{ij} is now the matrix coefficient for the system of equations corresponding to the total domain and Q_i are the forces only at the boundary of the total system. This result is justified by the fact that the summation extends to the variables not only at the interfaces of the sub-systems but also to the variables at the boundary of the total system. However, at the interfaces the forces are in pairs that cancel out. For example, for two sub-systems s and s' with a common boundary the generalized coordinates at the interface are q_i and the corresponding forces are Q_i and Q_i'. From the definition of the boundary force, the outward normal vectors for the domains with common boundaries are in opposite directions, hence

$$Q_i = -Q_i'$$

or (63)

$$Q_i + Q_i' = 0.$$

This leads to the cancellation of all the forces at the interfaces and the derived Eqs. (62) include only the forces at the boundary of the total system.

The procedure of dividing the domain of a system to sub-spaces is commonly used in approximate methods and a typical example is the identical procedure used for the analysis of a physical system by the finite element method.

3.2 Finite Element Method

A variety of approaches can be found under the name of the finite element method. Such approaches include the well known Galerkin methods, the Rayleigh-Ritz methods and many others which are usually modifications or derivatives of the ones mentioned. The formulation and derivation of the Galerkin method are well known and the method has been successfully applied to a variety of problems for obtaining numerical solutions. The Galerkin approach is usually referred to as the conventional finite element method in contrast to those which are based on modification of the Galerkin or non-conventional approaches. The intention here is to show that the conventional finite element method is a special application of the present generalized formulation. Consider the following approximation for the displacement field H_i

$$H_i(x,t) = a_0 + a_1 x + a_2 x^2 + a_3 x^3 + \ldots . \tag{64}$$

and the corresponding deformation field Θ

$$\Theta = a_1 + 2a_2 x + 3a_3 x^2 + \ldots . \tag{65}$$

where the a_i ($i = 0, 1, \ldots n$) are time dependent coefficients to be determined. Although the approximation given by Eq. (64) is restricted to one dimensional space, it can be easily extended to two or three dimensions since the derived formulations for approximate methods are of general form. In order to demonstrate the derivation of the matrix equation for the finite element method only a first order approximation will be considered here. Higher order approximations have been considered in previous studies [3,4] and their derivation is carried out in a similar way as the first order one. For a

first order approximation the derived finite element models correspond to linear element models with two degrees of freedom. Four such linear elements will be considered here. The first two are linear displacement models denoted by DFEM and DFET and correspond for the approximations given by Eqs. (44) and (55). The last two are conventional linear models in terms of the primitive variable Θ and are denoted by CFEM and CFET. The displacement models are derived from the fundamental form of the variational formulation and the conventional models from the complementary form.

3.2.1 Displacement Models

(a) DFEM

From Eq. (64) the approximation of the displacement field $H(x,t)$ for the linear element of length Δx is given by

$$H(x,t) = \left(1 - \frac{x}{\Delta x}\right) H_1(t) + \frac{x}{\Delta x} H_2(t) \tag{66}$$

where H_1 and H_2 are the nodal values of the displacement. They can be identified as the generalized coordinates q_1 and q_2 with the corresponding basis functions f_{x1} and f_{x2} given by

$$f_{x1} = \left(1 - \frac{x}{\Delta x}\right) \text{ and } f_{x2} = \frac{x}{\Delta x} \tag{67}$$

Then, according to Eq. (44), the approximation Eq. (66) is

$$H(x,t) = f_{xi}(x) H_i(t). \tag{68}$$

For the deformation Θ the approximation is evaluated from Eq. (67) as

$$\Theta(x,t) = \frac{1}{\Delta x} (H_2(t) - H_1(t)). \tag{69}$$

Note that within each element Θ varies only with time for the linear approximation of the displacement field. This is analogous to a constant strain element in mechanics.

The matrix coefficients of Eq. (54) are evaluated in terms of Eqs. (66) and (69) as

$$\begin{aligned} [d_{ij}] &= \frac{A\Delta x}{6k}\begin{bmatrix} 2 & 1 \\ 1 & 2 \end{bmatrix}, \quad [p_{ij}] = \frac{A}{\Delta x}\begin{bmatrix} 1 & -1 \\ -1 & 1 \end{bmatrix} \\ [v_{ij}] &= \frac{AV}{2k}\begin{bmatrix} -1 & 1 \\ -1 & 1 \end{bmatrix}, \quad [w_{ij}] = \frac{AK\Delta x}{6k}\begin{bmatrix} 2 & 1 \\ 1 & 2 \end{bmatrix} \end{aligned} \tag{70}$$

and

$$Q_i\Big|_{x=o} = Q_1 = -A\Theta, \quad Q_i\Big|_{x=\Delta x} = Q_2 = A\Theta$$

where A is the cross sectional area of the element, k is the diffusion coefficient and V the transport velocity. If one also assumes a linear approximation for the source term then S_i from Eq. (51) is evaluated as

$$\{S_i\} = \frac{A\Delta x}{6k}\begin{bmatrix}2 & 1\\ 1 & 2\end{bmatrix}\begin{Bmatrix}\dot{h}_1\\ \dot{h}_2\end{Bmatrix} = \frac{A\Delta x}{6k}\begin{Bmatrix}S_1\\ S_2\end{Bmatrix} \tag{71}$$

where $S_1 = 2\dot{h}_1 + \dot{h}_2$ and $S_2 = \dot{h}_1 + 2\dot{h}_2$. The matrix equation for the DFEM model is then assembled as

$$\begin{bmatrix}2 & 1\\ 1 & 2\end{bmatrix}\begin{Bmatrix}\dot{H}_1\\ \dot{H}_2\end{Bmatrix} + \left[\frac{3V_o}{W_o}\begin{bmatrix}-1 & 1\\ -1 & 1\end{bmatrix} + \frac{6}{W_o}\begin{bmatrix}1 & -1\\ -1 & 1\end{bmatrix} + K_o\begin{bmatrix}2 & 1\\ 1 & 2\end{bmatrix}\right]\begin{Bmatrix}H_1\\ H_2\end{Bmatrix} = \frac{6}{W_o}\begin{Bmatrix}-\Theta\\ \Theta\end{Bmatrix} + \begin{Bmatrix}S_1\\ S_2\end{Bmatrix} \tag{72}$$

The matrix equation, Eq. (72), has been derived in dimensionless form according to the transformations

$$\bar{x} = \frac{x}{L}, \quad \bar{t} = \frac{k}{L^2}t, \quad \Theta = \frac{C - C_o}{C_1 - C_o}, \quad \bar{H} = \frac{C_o}{C_1 - C_o}\frac{1}{L}H$$

$$W_o = \frac{\Delta x}{L}, \quad V_o = \frac{LV}{k}, \quad K_o = \frac{KL^2}{k}, \quad \bar{S}_i = \frac{L}{k}\frac{C_o}{C_1 - C_o}S_i. \tag{73}$$

Here L is a characteristic length and C_1 a constant reference value for C. The bar has been eliminated from Eq. (72) for simplicity.

(b) DFET model

If one now considers the approximation given by Eq. (55), then the linear approximation for $H(x,t)$ and $\Theta(x,t)$ will be given as

$$H(x,t) = \left(1 - \frac{x}{\Delta x}\right)\left(1 - \frac{t}{\Delta t}\right)H_1^1 + \left(1 - \frac{x}{\Delta x}\right)\frac{t}{\Delta t}H_1^2 + \frac{x}{\Delta x}\left(1 - \frac{t}{\Delta t}\right)H_2^1 + \frac{x}{\Delta x}\frac{t}{\Delta t}H_2^2 \tag{74}$$

and

$$\Theta(x,t) = \frac{1}{\Delta x}\left[\left(1 - \frac{t}{\Delta t}\right)(-H_1^1 + H_2^1) + \frac{t}{\Delta t}(-H_1^2 + H_2^2)\right] = \left(1 - \frac{t}{\Delta t}\right)\Theta^1 + \frac{t}{\Delta t}\Theta^2. \tag{75}$$

The generalized coordinates q_i^k and the corresponding function f_{xi} and g_n are identified as

$$q_1^1 = H_1^1,\ q_1^2 = H_1^2,\ q_2^1 = H_2^1,\ q_2^2 = H_2^2 \tag{76}$$

$$f_{x1} = 1 - \frac{x}{\Delta x},\ f_{x2} = \frac{x}{\Delta x} \tag{77}$$

$$g_1 = \left(1 - \frac{t}{\Delta t}\right),\ g_2 = \frac{t}{\Delta t}.$$

The matrix coefficients are evaluated from Eq. (58) and the matrix equation for the DFEMT model is assembled as

$$\left[\begin{bmatrix} -2 & -1 & 2 & 1 \\ -1 & -2 & 1 & 2 \\ -2 & -1 & 2 & 1 \\ -1 & -2 & 1 & 2 \end{bmatrix} + V_o\frac{\Delta t}{\Delta x}\begin{bmatrix} -2 & 2 & -1 & 1 \\ -2 & 2 & -1 & 1 \\ -1 & 1 & -2 & 2 \\ -1 & 1 & -2 & 2 \end{bmatrix} + 2\frac{\Delta t}{\Delta x^2}\begin{bmatrix} 2 & -2 & 1 & -1 \\ -2 & 2 & -1 & 1 \\ 1 & -1 & 2 & -2 \\ -1 & 1 & -2 & 2 \end{bmatrix}\right]\begin{Bmatrix} H_2^1 \\ H_2^1 \\ H_1^2 \\ H_2^2 \end{Bmatrix} = 2\frac{\Delta t}{\Delta x}\begin{Bmatrix} -(2\Theta^1 + \Theta^2) \\ (2\Theta^1 + \Theta^2) \\ -(\Theta^1 + 2\Theta^2) \\ (\Theta^1 + 2\Theta^2) \end{Bmatrix} \tag{78}$$

The two sets of equations given by Eqs. (72) and (78) represent the displacement finite element models for obtaining numerical solutions of the transport equation. Both models were derived from the fundamental form of the variational formulation as examples of approximate methods.

3.2.2 Conventional Models

(a) CFEM Model

The approximation for the transport variable Θ for the linear element of length Δx is given by

$$\Theta(x,t) = \left(1 - \frac{x}{\Delta x}\right)\Theta_1 + \frac{x}{\Delta x}\Theta_2 \tag{79}$$

where Θ_1 and Θ_2 are the nodal values of the transport variable. They can be identified as the generalized coordinates q_1 and q_2 with the corresponding functions f_{x1} and f_{x2} given by Eq. (67).

The matrix coefficients and the expressions for $\bar{D}$, $\bar{P}$, and $\bar{F}$, and $\bar{Q}_1$ are evaluated from Eqs. (40) through (43) and the resulting matrix equation is given by

$$\begin{bmatrix} 2 & 1 \\ 1 & 2 \end{bmatrix} \begin{Bmatrix} \Theta_1 \\ \Theta_2 \end{Bmatrix} + \left[\frac{3V_0}{W_0} \begin{bmatrix} -1 & 1 \\ -1 & 1 \end{bmatrix} + \frac{6}{W_0^2} \begin{bmatrix} 1 & -1 \\ -1 & 1 \end{bmatrix} + K_0 \begin{bmatrix} 2 & 1 \\ 1 & 2 \end{bmatrix} \right] \begin{Bmatrix} \Theta_1 \\ \Theta_2 \end{Bmatrix} = \frac{6}{W_0^2} \begin{Bmatrix} -(\Theta_2 - \Theta_1) \\ (\Theta_2 - \Theta_1) \end{Bmatrix} + \begin{Bmatrix} S_1 \\ S_2 \end{Bmatrix} \tag{80}$$

The above equation has resulted from the complementary form of the variational formulation and is identical to the finite element equations obtained by the conventional Galerkin method. Furthermore the matrix coefficients are identical to the ones given by Eqs. (70).

(b) CFET Model

The linear approximation for the transport variable Θ is given by

$$\Theta(x,t) = \left(1 - \frac{x}{\Delta x}\right)\left(1 - \frac{t}{\Delta t}\right)\Theta_1^1 + \left(1 - \frac{x}{\Delta x}\right)\frac{t}{\Delta t}\,\Theta_1^2 + \frac{x}{\Delta x}\left(1 - \frac{t}{\Delta t}\right)\Theta_2^1 + \frac{x}{\Delta x}\frac{t}{\Delta t}\,\Theta_2^2 \tag{81}$$

As for the previous approximations the generalized coordinates can be identified as

$$q_i^j = \Theta_i^j, \quad i = 1, 2, \quad j = 1, 2 \tag{82}$$

and the corresponding functions f_n and g_n are given by Eqs. (76) and (77). The matrix coefficients are evaluated in terms of Eq. (81) and the matrix equation for the CFET model can be derived from Eq. (78) by replacing the nodal unknowns H_i^j by Θ_i^j.

The four finite element models presented in this section can be grouped into two types of models which correspond to the general approximation given by Eqs. (44) and (55). The first type can be represented by the following generalized equation

$$d_{ij}\dot{q}_i + (v_{ij} + p_{ij} + w_{ij})q_j = Q_i + S_i \tag{83}$$

where the matrix coefficients are given by Eqs. (70) and the generalized coordinates are identified as

$$\begin{aligned} &\text{DFEM model}: \quad q_i = H_i, \quad i = 1, 2 \\ &\text{CFEM model}: \quad q_i = \Theta_i, \quad i = 1, 2. \end{aligned} \tag{84}$$

For the DFEM model Eq. (83) should be used together with the constraint

$$\Theta_i = \frac{1}{\Delta x}(H_{i+1} - H_i) \tag{85}$$

The second type of models can be represented by

$$[d_{ijkl} + v_{ijkl} + p_{ijkl} + w_{ijkl}]\, q_i^j = Q_i^k + S_i^k \tag{86}$$

where the matrices are given by Eqs. (78) and the generalized coordinates are identified as

$$\text{DFET model: } q_i^j = H_i^j \quad i = 1, 2, \quad j = 1, 2$$
$$\text{CFET model: } q_i^j = \Theta_i^j \quad i = 1, 2, \quad j = 1, 2 \tag{87}$$

and for the DFET model Eq. (83) should be used together with the constraint given by Eq. (75). In the following table the four models are presented in summary.

Table 1

Approximation	Model	Generalized Coordinates	Type of Matrix Equations
Only for spatial coordinates S-type	DFEM	$q_i = H_i$	Ordinary Differential Eq. (83)
	CFEM	$q_i = \Theta_i$	
For both spatial and time coordinates S-T-type	DFET	$q_i^j = H_i^j$	Algebraic Eq. (86)
	CFET	$q_i^j = \Theta_i^j$	

Both types of models have been used to solve problems of transport phenomena and some examples will be given later in this study. From these examples a realistic comparison between models and also an evaluation of the models is possible.

The generalized variational formulations and the derived approximate methods presented here represent a unified approach for describing transport phenomena. Some of the advantages of this unified approach are as follows:

- The variational formulation is problem independent.
- The presentation of the transport equation by generalized coordinates simplifies the complexity of the equation.
- The Lagrangian type of equations are most suitable for obtaining approximate solutions.
- The finite element method can be derived directly as a special application for approximate solutions.

- The derived finite element models can be represented by one generalized model.

- The displacement models are most suitable for solving problems with discontinuities.

In the following a number of numerical solutions will be presented for specific boundary value problems and the error behavior of these numerical solutions will be investigated.

4. NUMERICAL APPLICATIONS

The transport equation is considered in this section as describing convective heat transfer. With this choice of a transport process, one can identify the transport parameter Θ to represent temperature defined by

$$\Theta = \frac{T - T_0}{T_0}$$

where T and T_0 are absolute temperature at the present and reference states respectively and the transport displacement will be then called the heat displacement [3].

Convective heat transfer provides a good test case for numerical solutions since a variety of boundary conditions can be considered. Before numerical solutions to specific problems are presented it is appropriate to investigate the stability and the error behavior of the four element models. Since it is necessary to use a numerical scheme to approximate the time derivatives of the S-type models, a finite difference scheme is chosen for that purpose. The scheme is known as the backward finite difference approximation. It is an implicit, unconditionally stable scheme and the general approximation for the first derivative is given by the following series expansion [7]

$$\frac{dy(t_i)}{dt} = \frac{1}{\Delta t} \sum_{j=0}^{n} a_j y(t_{i-j}) + O(\Delta t^{n-1}) \tag{88}$$

where a_j are constant coefficients and their values are given for up to a fourth order approximation in Table 2.

Table 2

Order of Approximation		a_0	a_1	a_2	a_3	a_4	a_5
First,	$n = 1$	1.0	−1.0	0.0	0.0	0.0	0
Second,	$n = 2$	1.5	−2.0	0.5	0.0	0.0	0
Third,	$n = 3$	11./6.	−3.0	1.5	−1./3.	0.0	0
Fourth,	$n = 4$	25./12.	−4.0	3.0	−.4/3.	0.25	0

The error analysis of the numerical solution of a particular problem will be presented in the following section and some criteria for convergence and error estimates will be discussed.

4.1 Problem Definition

One representative example of transport phenomena is the convection and diffusion of heat by a moving fluid. The governing equation for the one dimensional case of convection-diffusion is given by

$$\frac{\partial \Theta}{\partial t} + V_o \frac{\partial \Theta}{\partial x} - D_o \frac{\partial^2 \Theta}{\partial x^2} = 0 \tag{89}$$

where Θ is the dimensionless temperature, V_o is the constant flow velocity and D_o a constant diffusivity. It has been also assumed that there is no heat sources or sink involved in the fluid. The boundary and initial conditions are as follows

$$\begin{aligned} &\Theta(x,0) = 0.0, \quad 0.0 \leqslant x \leqslant L \\ &\Theta(0,t) = 1.0, \quad 0.0 \leqslant t \leqslant t_f \\ &\Theta(L,t) = 0.0, \quad 0.0 \leqslant t \leqslant t_f \end{aligned} \tag{90}$$

where L is a finite characteristic length approximating infinity. The analytical solution to the above problem is given by

$$\Theta(x,t) = 1/2\left[\exp\left[\frac{V_o x}{D_o}\right] \operatorname{erfc}\left[\frac{x + V_o t}{2\sqrt{D_o t}}\right] + \operatorname{erfc}\left[\frac{x - V_o t}{2\sqrt{D_o t}}\right]\right]. \tag{91}$$

The solution of the convection-diffusion equation in the semi-infinite space is a typical example for testing numerical solutions and studying error behavior. Its numerical solution is challenging, especially for small values of the diffusion coefficient ($D_o << V_o$), where the discontinuities in the temperature field are difficult to simulate numerically.

4.2 Error Analysis

Numerical solutions of the above problem are obtained by the four finite element models previously derived and these numerical solutions are compared to the analytical one, Eq. (91), in order to investigate the error behavior. For the S-type models (DFEM and CFEM) a first order backward finite difference scheme is chosen to approximate the time derivative. This is an appropriate choice since the

order of accuracy of the first order scheme is the same as the accuracy of the linear in time approximation of the S-T-type models (DFET and CFET).

The error of the numerical solution is the average error E_n over the entire length L at a particular time level and it is evaluated by the following relation

$$E_n = \frac{1}{N} \sum_{i=1}^{N} |\Theta - \Theta_i| \tag{92}$$

where N is the number of elements used for the space discritization and $|\Theta - \Theta_i|$ is the absolute local error. For illustrating numerical results, the characteristic length $L = 1$ is divided into a uniform mesh with NE elements and $NP = NE + 1$ nodal points (degrees of freedom), and the dimensionless element length then equals to $1/NE$. Three sets of values for the constants V_o and D_o will be used in investigating the convergence and error of the numerical solutions. These values are shown in Table 3 and each set is used for all four models.

Table 3

Case	V_o	D_o	Name
I	1.0	0.001	Convection
II	1.0	1.0	Convection-Diffusion
III	0.0	1.0	Diffusion

For each of these values four sets of results will be presented for all four models. The first set of results is obtained for a constant value of Δx and variable Δt (Table 4) and the second set is obtained for constant Δt and variable Δx (Table 5). The third for constant values of the ratio $\Delta t/\Delta x$ (Table 6) and the fourth set for constant values of the ratio $\Delta t/\Delta x^2$ (Table 7).

Table 4

NE	Δx	Δt	$M_1 = \Delta t/\Delta x$	$M_2 = \Delta t/\Delta x^2$
20	1/20.0	0.0001	0.002	0.04
		0.00025	0.005	0.10
		0.0005	0.010	0.20
		0.00125	0.025	0.50
		0.0050	0.100	2.00
		0.0100	0.200	4.00
		0.0125	0.250	5.00
		0.0200	0.400	8.00
		0.0250	0.500	10.00
		0.0500	1.000	20.00

Table 5

Δt	NE	Δx	$M_1 = \Delta t/\Delta x$	$M_2 = \Delta t/\Delta x^2$
0.005	5	1/5.0	0.025	0.125
	10	1/10.0	0.050	0.500
	20	1/20.0	0.100	2.000
	30	1/30.0	0.150	4.500
	40	1/40.0	0.200	8.000
	50	1/50.0	0.250	12.500
	60	1/60.0	0.300	18.000
	80	1/80.0	0.400	32.000
	100	1/100.	0.500	50.000
	200	1/200.0	1.000	200.00

Table 6

NE	Δx	Δt	$M_1 = \Delta t/\Delta x$	$M_2 = \Delta t/\Delta x^2$
10	0.100000	0.02500		2.50
20	0.05000	0.01250		5.00
40	0.02500	0.00625		10.00
50	0.02000	0.00500	0.25	12.50
80	0.01250	0.00312		20.00
100	0.01000	0.00250		25.00

Table 7

NE	Δx	Δt	$M_1 = \Delta t/\Delta x$	$M_2 = \Delta t/\Delta x^2$
10	0.1	0.0250	0.250	
20	0.050	0.00625	0.125	
40	0.0250	0.00156	0.063	2.5
50	0.0200	0.00100	0.050	
80	0.0125	0.00040	0.031	
100	0.0100	0.00025	0.025	

In all of the figures the average error is presented at three time levels. This is necessary in order to investigate the error behavior throughout the time integration domain. The first set, Figs. 1-3, the value of NE is constant ($NE = 20$) and the time step Δt was given values $0.0001 \leqslant \Delta t \leqslant 0.05$. The corresponding values for $\Delta t/\Delta x$ and $\Delta t/\Delta x^2$ are given in Table 4. The second set of results are given in Figs. 4-6 where Δt is constant ($\Delta t = 0.005$) and NE was given values $5 \leqslant NE \leqslant 200$. Table 5 contains the values for Δx and the corresponding values of $\Delta t/\Delta x$ and $\Delta t/\Delta x^2$.

4.2.1 Displacement Models (DFET, DFEM)

In Figs. 1a through 6a results for the average errors E_n are given for the two displacement models and for the three cases of the coefficients V_o and D_o. In the first three figures (1a, 2a, 3a), the error E_n is given as a function of Δt and the next three figures, (4a, 5a, 6a), E_n is given as a function of NE. The error behavior in all six figures follows a similar pattern. As Δt or NE increases there is initially a reduction in the error of the numerical solutions, and a minimim error is reached. With further increases of Δt or NE the error starts to increase but the rate of change is smaller than before the minimum was reached. The difference between the values of the error for the two models is very small for small values of Δt but it becomes noticeable as Δt increases with the DFET model being the more accurate one. Similar observations can be made for the error behavior with respect to NE. The error behavior in all six figures shows a nonuniform convergence as Δt increases or Δx decreases. This pattern is not unusual since only Δt or Δx is changed while Δx or Δt remains constant respectively. Certain observations can be made from the results presented in the six figures.

- There is an optimum combination of Δt and Δx for minimum error for both models.
- To the left of the optimum point the error of the DFEM model is smaller than the error for the DFET model. The order of accuracy is reversed just before the optimum point and the difference in error between the two models becomes larger.
- For small values of the coefficient D_o, ($D_o << V_o$), there are larger differences in error between the two models with the DFET being more accurate.
- As time progresses the value of the minimum error decreases and the optimum points are translated to the right
- For large values of Δt or NE the error increases monotonically with time.
- There seems to be an area where the error curves for different time levels intersect, indicating that a constant error value can be achieved for certain combinations of Δt and Δx throughout the time domain. This is more pronounced in Figs. 4a-6a.

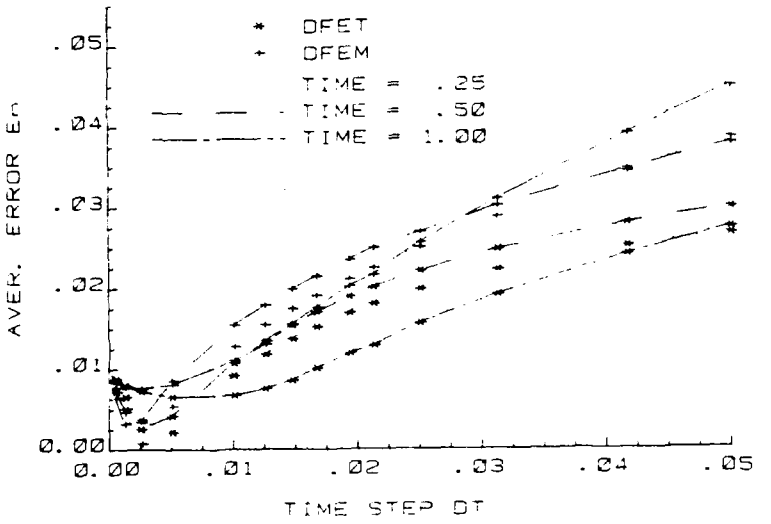

(a)

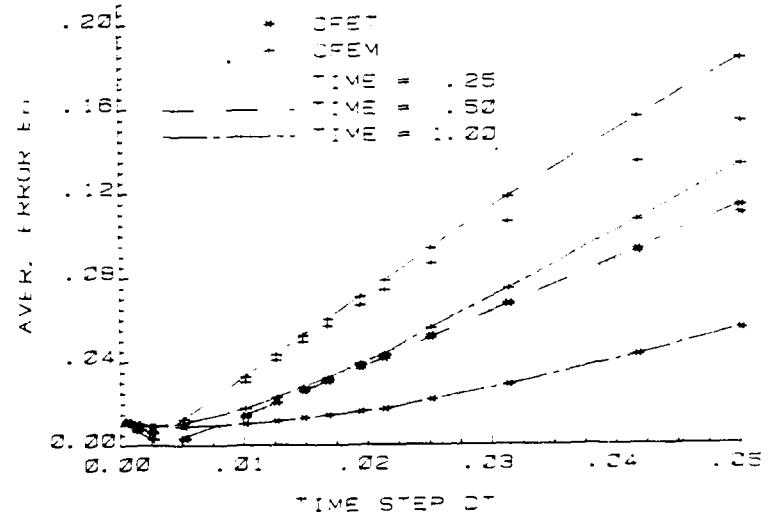

(b)

Fig. 1 — Average error for constant Δx, ($V_0 = 1.0$, $D_0 = 0.001$): (a) Displacement models and (b) Conventional models

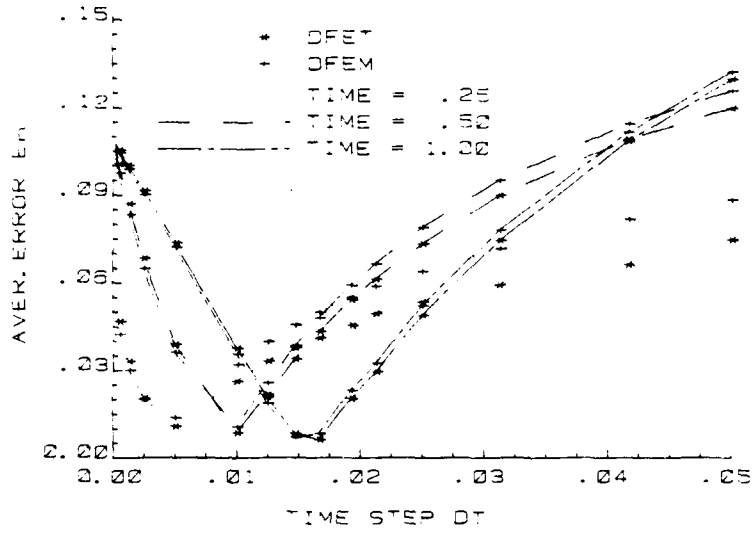

(a)

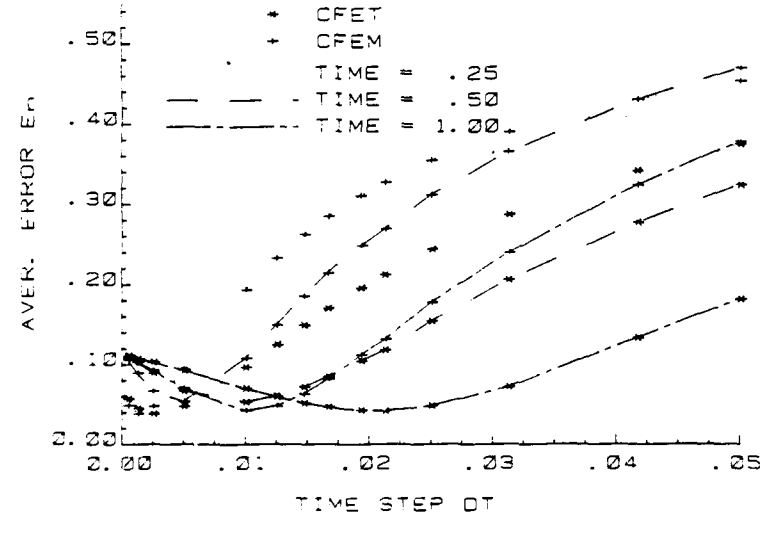

(b)

Fig. 2 — Average error for constant Δx, ($V_0 = 1.0$, $D_0 = 1.0$):
(a) Displacement models and (b) Conventional models

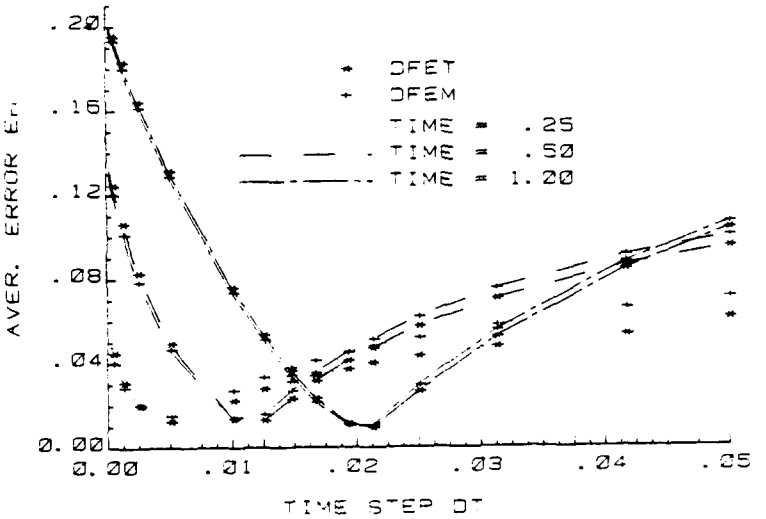

(a)

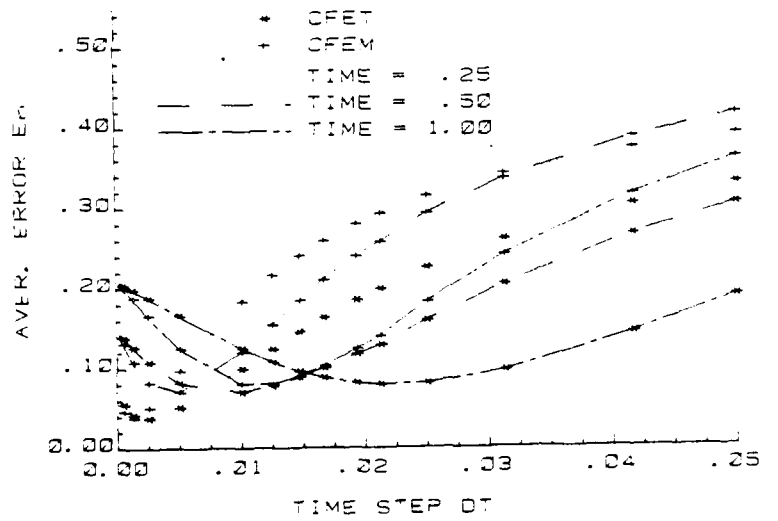

(b)

Fig. 3 — Average error for constant Δx, ($V_0 = 0.0$, $D_0 = 1.0$): (a) Displacement models and (b) Conventional models

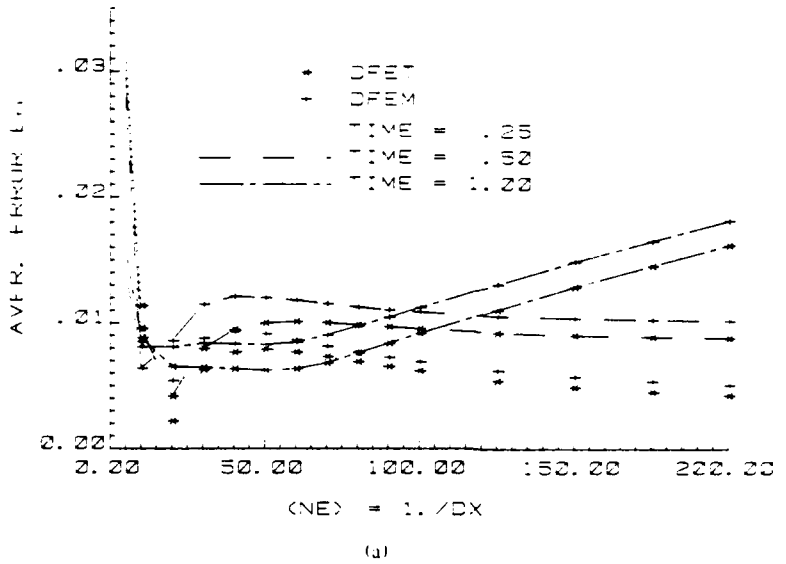

(a)

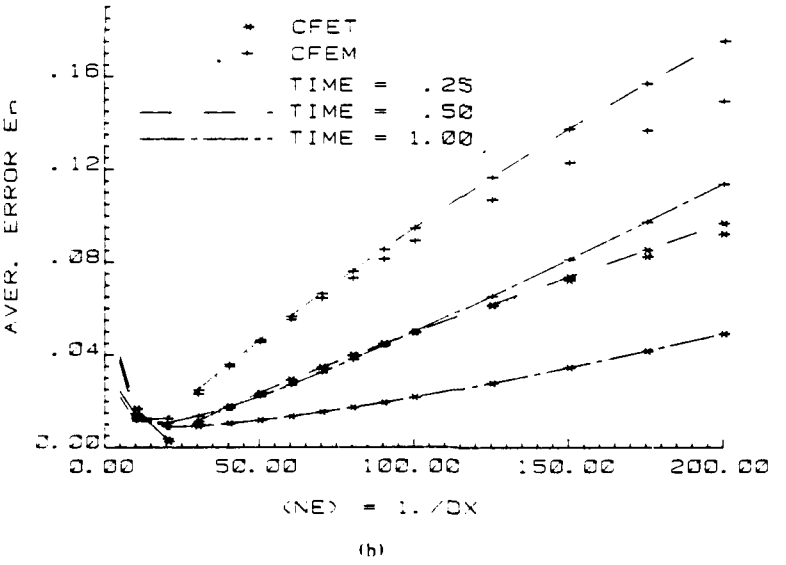

(b)

Fig. 4 — Average error for constant Δt, ($V_0 = 1.0$, $D_0 = 0.001$): (a) Displacement models and (b) Conventional models

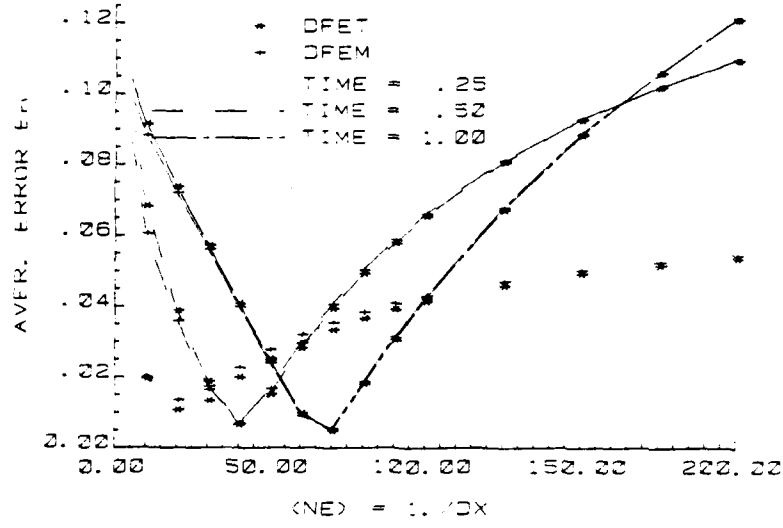

(a)

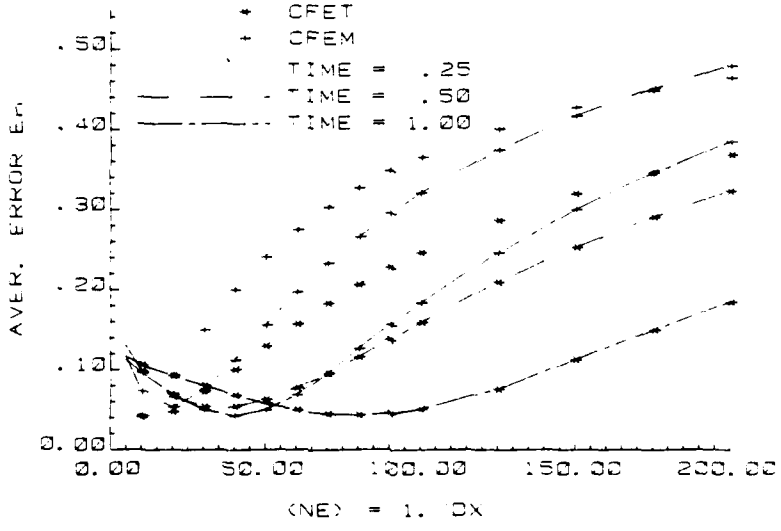

(b)

Fig. 5 — Average error for constant Δt, ($V_0 = 1.0$, $D_0 = 1.0$): (a) Displacement models and (b) Conventional models

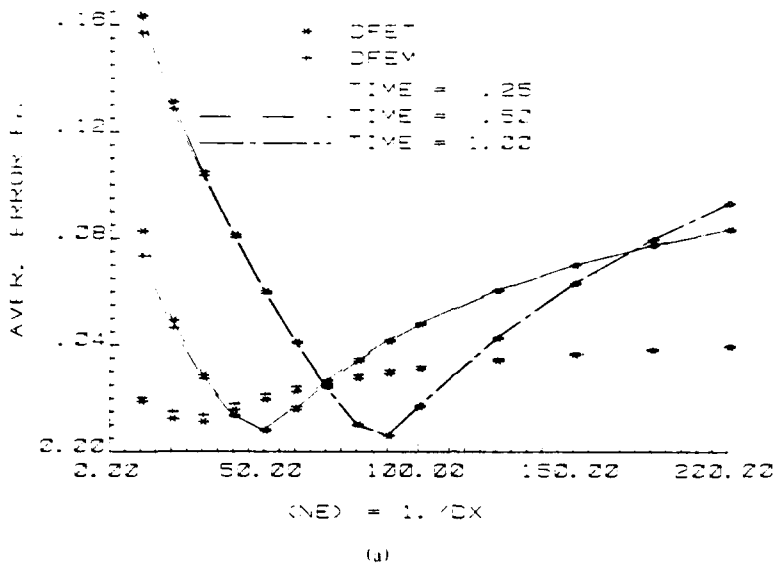

(a)

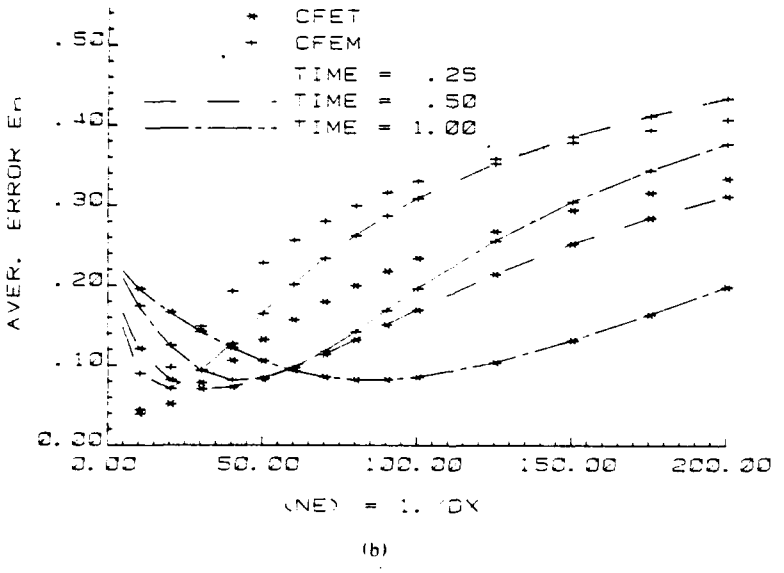

(b)

Fig. 6 — Average error for constant Δt, ($V_0 = 0.0$, $D_0 = 1.0$): (a) Displacement models and (b) Conventional models

The similarities observed in error behavior may lead to some optimum combination of Δt and Δx for error control of the numerical solutions.

4.2.2 Conventional Models (CFET, CFEM)

In Figs. 1b-6b results are given for the two conventional finite element models and for the same set of values of the coefficients D_o and V_o as before. The error behavior with respect to Δt or Δx shows similarities to the error behavior of the displacement models but there is no uniformity in the error behavior. For example, for either constant Δt or Δx the error values reach a minimum but as time progresses these minimum error values do not follow a regular pattern as for the displacement models. Furthermore, the difference in error between the CFET and the CFEM model is much larger than the difference between the DFET and DFEM models.

Another observation is the difference in error between the displacement and conventional models. In all six figures the error values for the displacement models are two to three times smaller than the corresponding values of the conventional models. For example, in Figs. 2a and 2b at small values of Δt the error is about the same, but as Δt increases ($\Delta t > 0.01$, $M_1 > .2$) the error for the conventional models, Fig. 2b, becomes much larger. This is due mainly to the error involved in applying the boundary conditions ($x = L$), and also due to the absence of the boundary forces. In the case of the conventional models the boundary forces are zero for prescribed temperature at the boundary. Furthermore, as was mentioned earlier in this study, the presence of space derivatives in the complementary formulation is the main drawback of the conventional models and they contribute to the larger error of these models. In the following discussion certain examples will be used to demonstrate this defficiency.

The previously made observations on the patterns of the error behavior suggest that optimum combinations of Δt and Δx can be defined for error control of the numerical solution. These combinations can be based on optimum values of the ratio $M_1 = \Delta t/\Delta x$ or the ratio $M_2 = \Delta t/\Delta x^2$. Typically for a second order equation, such as the transport equation, the ratio M_2 is the parameter for error and stability control. The value of this parameter, when it is kept within certain limits, guarantees accuracy and stability of the numerical solution [8].

A careful examination of the results for the error, shown in Figs. 1a-6a, and the values of M_2 from Tables 4 and 5 which correspond to minimum error shows that there is an inconsistency. For example, at time $t = 0.5$ Table 4 and Fig. 2a show minimum error at $M_2 = 5.00$, ($\Delta t = 0.0125$), but from Table 5 and Fig. 5a the minimum error is at $M_2 = 12.5$ ($NE = 50$). What appears to be an inconsistency in the behavior of the displacement models, with respect to the parameter M_2, leads to the observation that M_2 might not be the right parameter for error control of the numerical solution. In contrast an examination of the error with respect to M_1 shows that at time $t = 0.5$ the minimum values of the error, Figs. 2a and 5a, correspond to the same value of the parameter M_1. In fact for each value of the parameter M_1 the corresponding error values are about the same in all six figures.

In order to study the dependence of the numerical solution error on the two parameters M_1 and M_2 further analysis is needed. The error of the numerical solution now is investigated for some constant values of the two parameters. Results are given for all four models and it is shown that uniform convergence can be achieved either for constant M_1 or M_2. Furthermore, it is shown that uniform convergence does not always correspond to minimum error.

4.3 Convergence of the Numerical Solution

Numerical experiments on the error of the solutions in the previous section show that nonuniform convergence is obtained when either Δt or Δx alone is the dependent variable. It was also observed that minimum error could be achieved for some optimum combinations of the two variables Δt and Δx. It is a well known fact that in order to achieve uniform convergence both Δt and Δx should be the dependent variables with the condition that the ratio $\Delta t/\Delta x$ or $\Delta t/\Delta x^2$ is kept constant. The results for the average error E_n in this section will show that uniform convergence is obtained for both the displacement and conventional models when M_1 or M_2 is kept constant. Some representative values of M_1 and M_2 are given in Tables 8 and 9, with the corresponding values of Δt and Δx, for the four models. Numerical results are presented in Figs. 7 through 15, for all models and all cases as before, and for two values of each of the parameters M_1 and M_2.

Results are given in the first three figures, Figs. 7a-9a, for the displacement models for constant $M_1 = 0.25$ and in the next three, Figs. 7b-9b, results are given for $M_2 = 2.5$. The uniform conver-

Table 8

M_1	M_2	Δx	Δt
	2.50	0.10000	0.02500
	5.00	0.0500	0.01250
0.25	10.00	0.0250	0.00625
	12.50	0.0200	0.00500
	20.00	0.0125	0.00312
	25.00	0.0100	0.00250
	5.00	0.1000	0.05000
0.50	10.00	0.0500	0.02500
	20.00	0.0250	0.01250
	40.00	0.0125	0.00625
	50.00	0.0100	0.00500

Table 9

M_1	M_2	Δx	Δt
0.250		0.1000	0.02500
0.125		0.0500	0.00625
0.063	2.5	0.0250	0.00156
0.050		0.0200	0.00100
0.031		0.0125	0.00039
0.025		0.0100	0.00025
0.500		0.1000	0.05000
0.250		0.0500	0.01250
0.125	5.0	0.0250	0.00312
0.100		0.0200	0.00200
0.063		0.0125	0.00078
0.050		0.0100	0.00050

gence of the numerical solution is obvious for either of the parameters M_1 or M_2. Examining each pair of figures (Figs. 7a and b, 8a and b, and 9a and b) which correspond to the same set of the parameters V_o and D_o one can observe the effect of M_1 and M_2 in the error of the solution for the displacement models. For both M_1 and M_2 the error reaches a constant value but these constant error values are smaller for the case of constant M_1 than for the case of constant M_2. This becomes more evident as the value of D_o increases. For example, in Figs. 8a and 8b, for each value of Δx the corresponding error value is much larger for constant M_2 than for constant M_1. Furthermore, the corresponding value of Δt for each Δx, Table 8, is less for the case of $M_2 = 2.5$ than for $M_1 = 0.25$. This behavior of error is consistant with the error behavior of the previous section where it was shown that a smaller value of Δt for a particular value of Δx does not always mean smaller error.

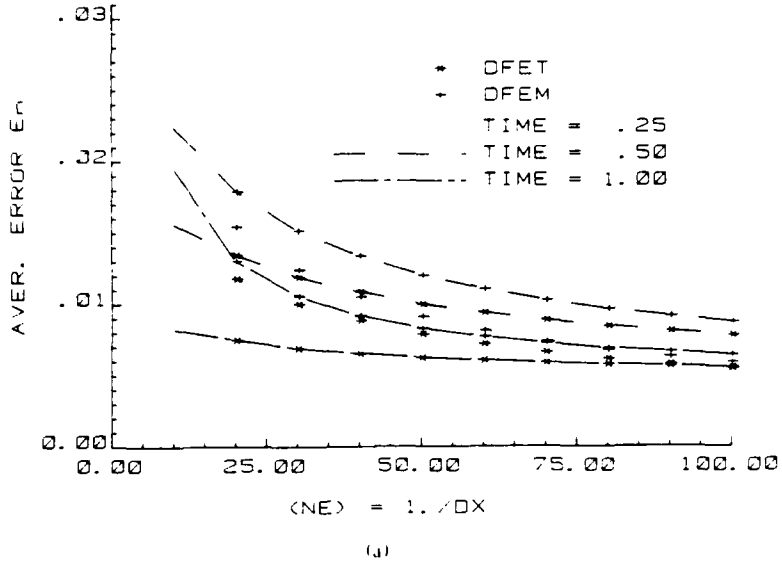

(a)

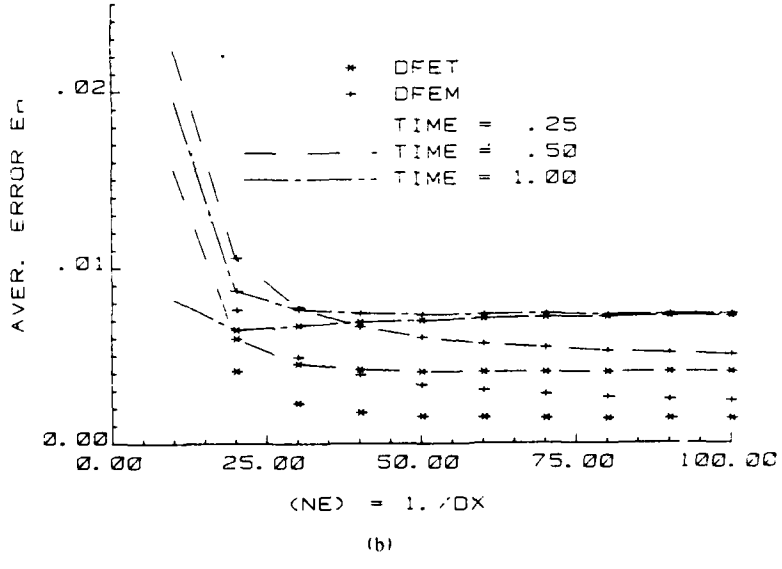

(b)

Fig. 7 — Average error for the displacement models, ($V_0 = 1.0$, $D_0 = 0.001$): (a) $M_1 = 0.25$ and (b) $M_2 = 2.5$

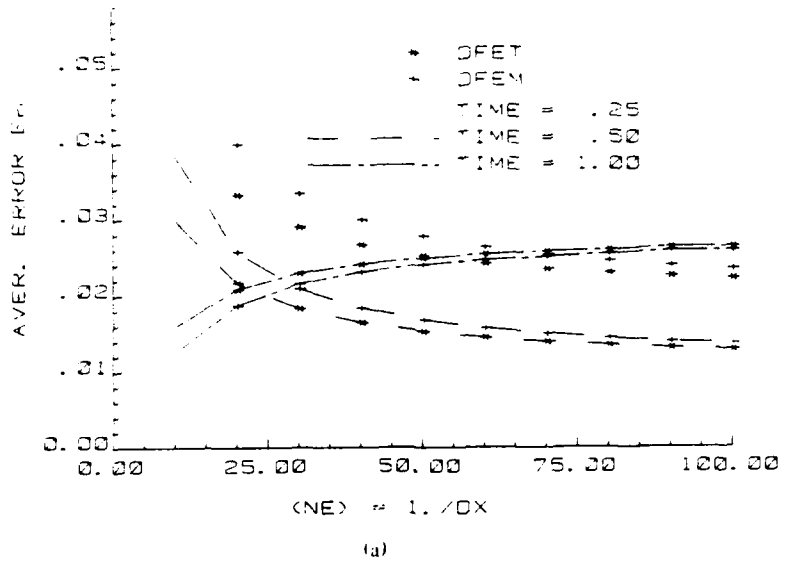

(a)

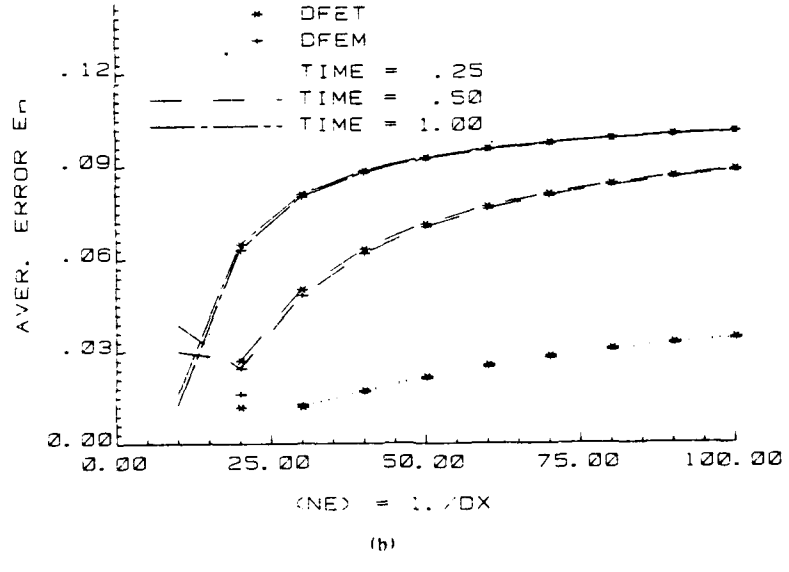

(b)

Fig. 8 — Average error for the displacement models, ($V_0 = 1.0$, $D_0 = 1.0$): (a) $M_1 = 0.25$ and (b) $M_2 = 2.5$

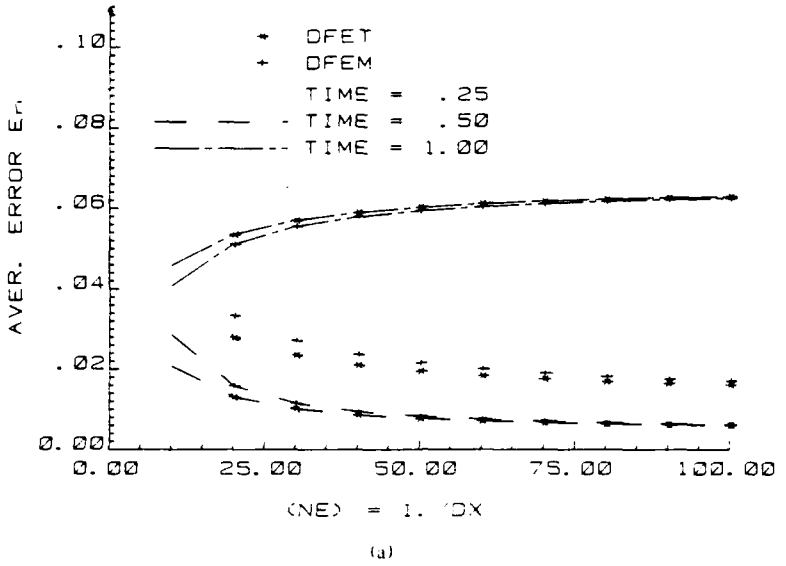

(a)

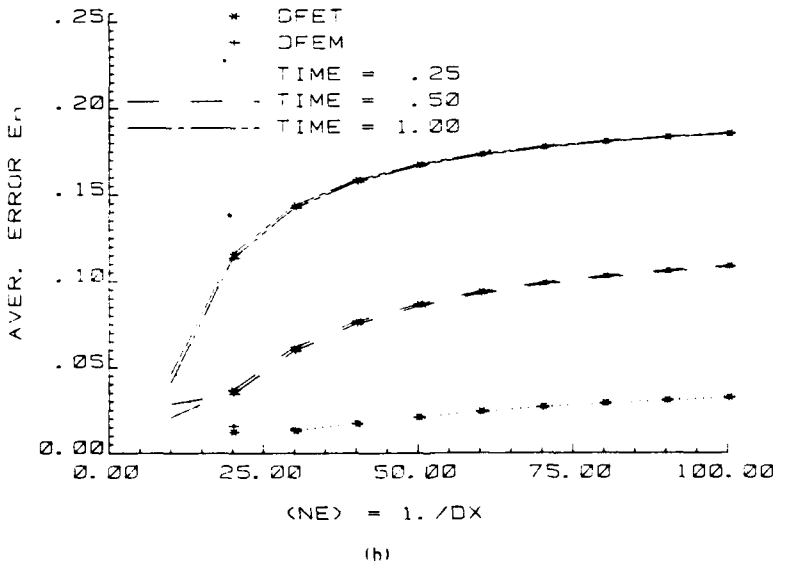

(b)

Fig. 9 — Average error for the displacement models, ($V_0 = 0.0$, $D_0 = 1.0$): (a) $M_1 = 0.25$ and (b) $M_2 = 2.5$

Since in any numerical solution we are concerned not only with the convergence but also with the amount of error involved and the economy with which the solution is obtained, it is obvious that in the case of the displacement models the parameter for error control should be M_1 and not M_2. In the next six figures, Figs. 10-12 results are given for the conventional models and for the same cases as above. Again uniform convergence is obtained for both parameters M_1 and M_2 but the error values for constant M_1 are now larger than for constant M_2. This is the opposite from what was the case for the displacement models. Furthermore, the difference in error between the two conventional models, CMET and CFEM, is much larger for $M_1 = 0.25$ than for $M_2 = 2.5$. It is obvious from the six figures that for the conventional models the dominant parameter is M_2 and not M_1. Also for the larger values of Δt ($M_1 = 0.25$) the numerical solution is more sensitive to the type of time integration scheme used.

It appears that for the displacement models the correct parameter for error control is the ratio M_1 and for the conventional models, the correct parameter is the ratio M_2. This can be justified first by the type of equation involved in each of the formulations and second by the results obtained for the average error of the numerical solutions. The equation for which numerical solutions are sought through the displacement models Eq. (8), does not contain second order space derivatives of the transport variable and only the ratio $\Delta t/\Delta x$ appears in the approximations of this equation. In contrast the equation for which numerical solutions are sought through the conventional models, Eq. (3), does contain second order derivatives, hence the ratio $\Delta t/\Delta x^2$ appears in the approximation of this equation. The results presented in this section are in full agreement with this reasoning.

In the last part of this section two more sets of figures are given for different values of the parameters M_1 and M_2. These sets of figures together with Figs. 7a-9a and Figs. 10b-12b can be used to evaluate and compare the displacement and conventional models. For the displacement models, Figs. 7a-9a and Figs. 13a-15a the error increases as the value of M_1 increases from 0.25 to 0.5. A similar behavior is observed for the conventional models as M_2 increases from 2.5 to 5.0. Comparing now Figs. 7a through 9a to Figs. 10b through 12b and Figs. 13a through 15a to Figs. 13b through 15b one can observe that the displacement models consistently result in smaller error values than the conven-

tional ones, especially for large values of Δx (small NE). Furthermore, the smaller error values are obtained by the displacement models with a larger time step. For a given value of Δx, say $\Delta x = 0.025$, the values of Δt which correspond to $M_1 = 0.25$ (DFET and DFEM) and $M_2 = 2.5$ (CFET and CFEM) are $\Delta t_1 = 0.00625$ and $\Delta t_2 = 0.00156$ respectively. This can be easily observed from the two Tables 8 and 9 and from Figs. 7 through 15.

The following general observations can be made regarding the error behavior of the numerical models.

- Uniform convergence is obtained for all models only when the ratio M_1 or the ratio M_2 is kept constant.
- Uniform convergence does not automatically guarantee minimum error.
- For the DFET and DFEM models the minimum error is obtained when the control parameter is M_1.
- For the CFET and CFEM models the minimum error is obtained when the control parameter is M_2.
- Of the two time integration schemes used, the finite element in time is consistantly more accurate in all cases.
- The displacement models are computationally more efficient overall since they can achieve smaller error than the conventional ones by using larger time steps.
- For all of the models the error decreases significantly up to $NE = 40$ and an increase of NE beyond this value has only small effect on the numerical solution.

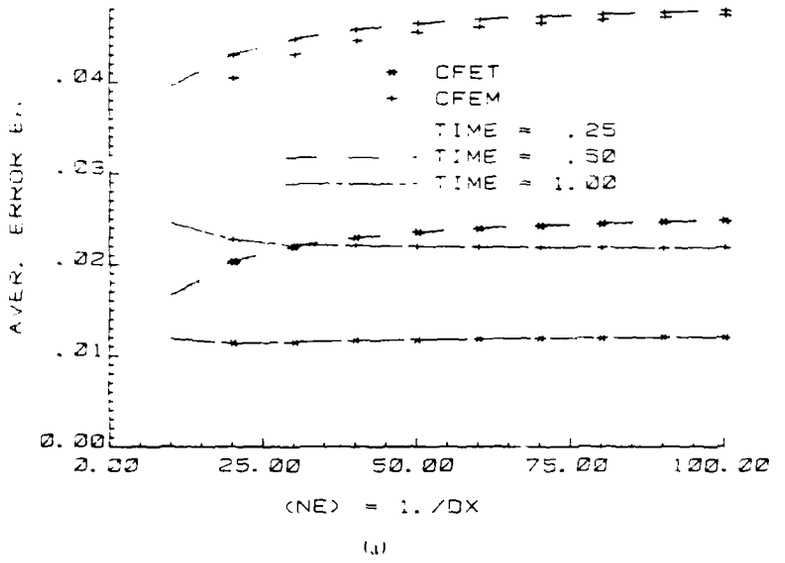

(a)

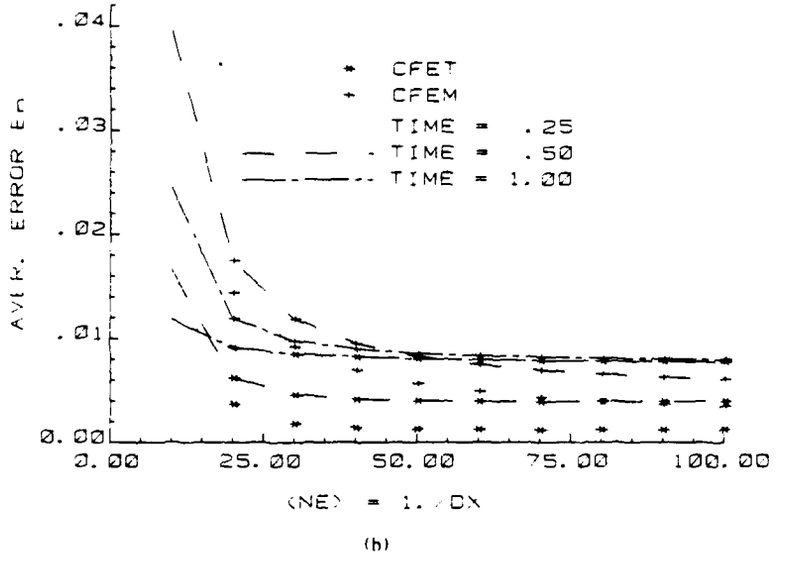

(b)

Fig. 10 — Average error for the conventional models, ($V_0 = 1.0$, $D_0 = 0.001$): (a) $M_1 = 0.25$ and (b) $M_2 = 2.5$

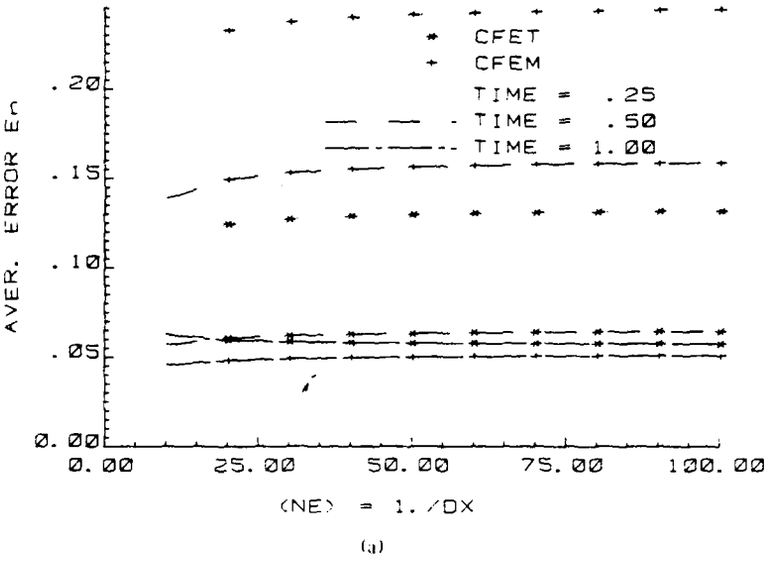

(a)

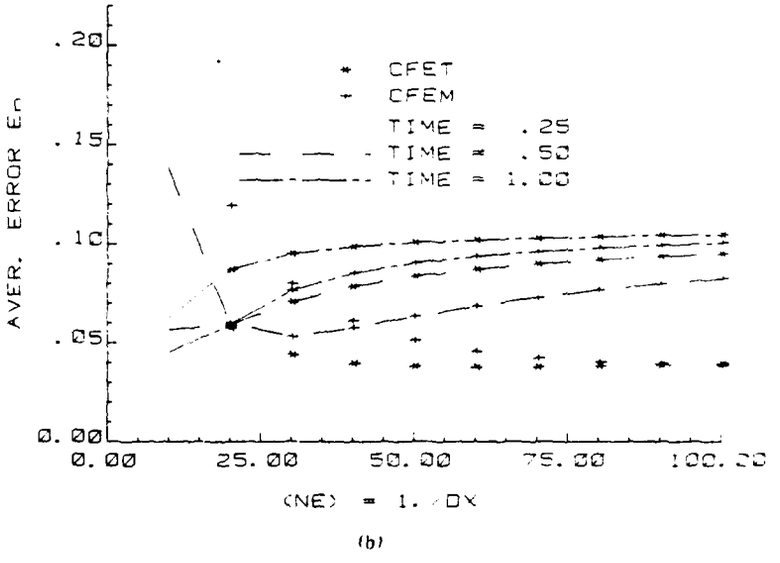

(b)

Fig. 11 — Average error for the conventional models, ($V_0 = 1.0$, $D_0 = 1.0$): (a) $M_1 = 0.25$ and (b) $M_2 = 2.5$

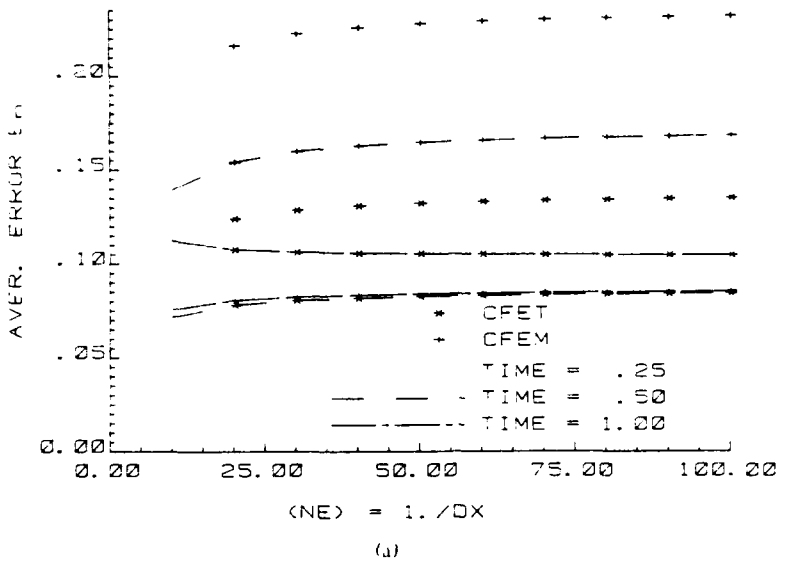

(a)

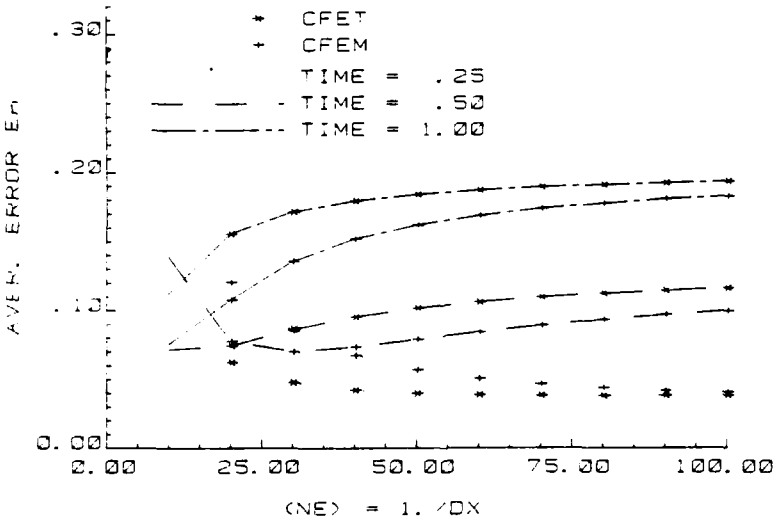

(b)

Fig. 12 — Average error for the conventional models, ($V_0 = 0.0$, $D_0 = 1.0$): (a) $M_1 = 0.25$ and (b) $M_2 = 2.5$

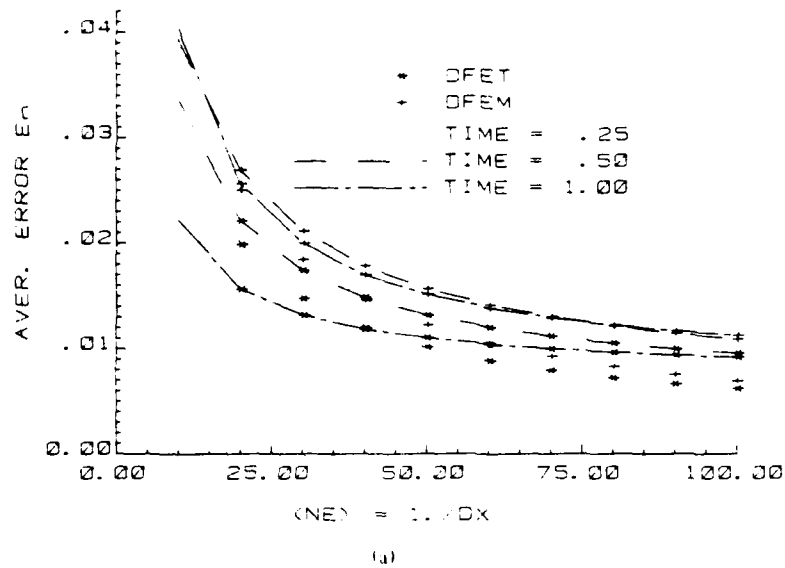

(a)

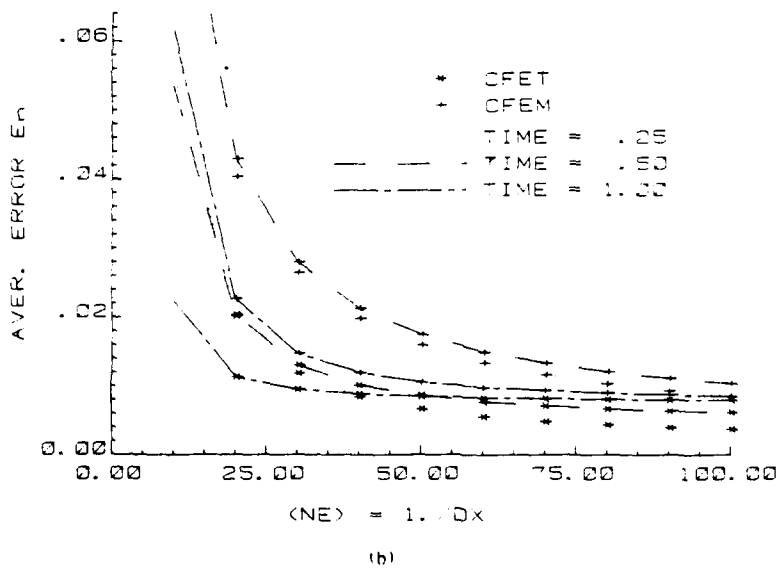

(b)

Fig. 13 — Average error ($V_0 = 1.0$, $D_0 = 0.001$): (a) Displacement models $M_1 = 0.5$ and (b) Conventional models $M_2 = 5.0$

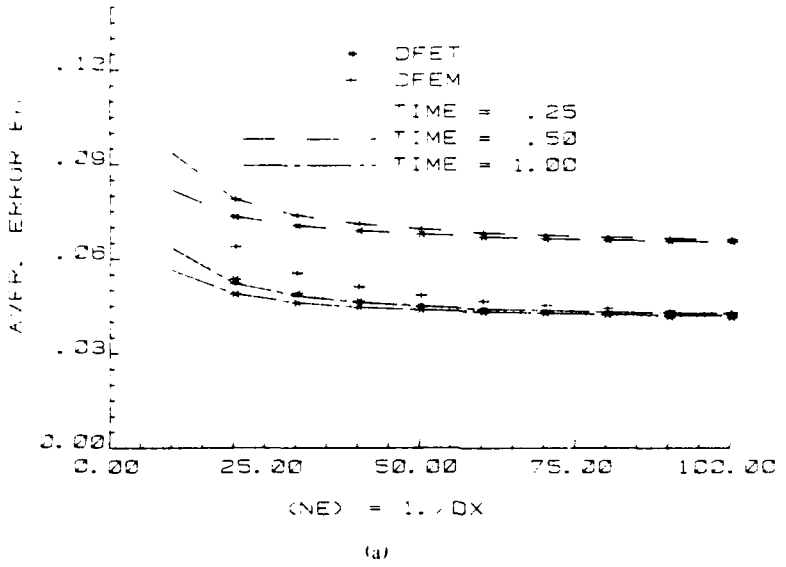

(a)

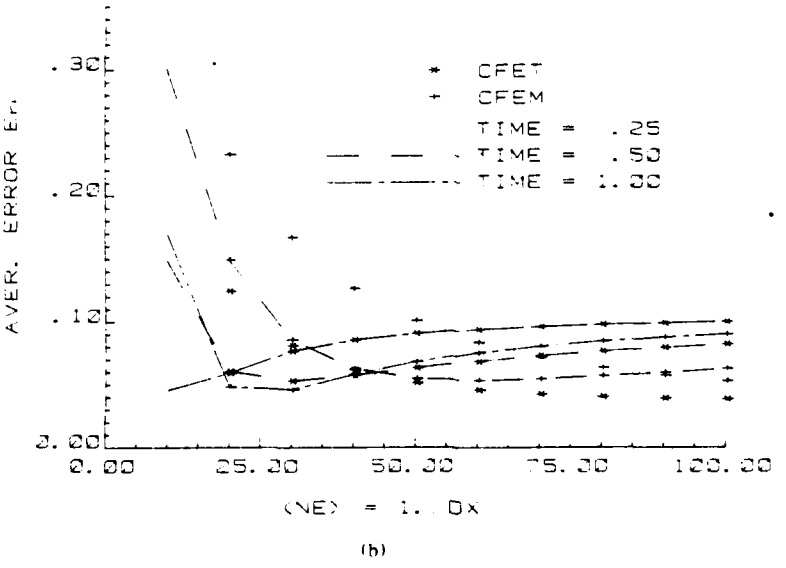

(b)

Fig. 14 — Average error ($V_0 = 1.0$, $D_0 = 1.0$): (a) Displacement models $M_1 = 0.5$ and (b) Conventional models $M_2 = 5.0$

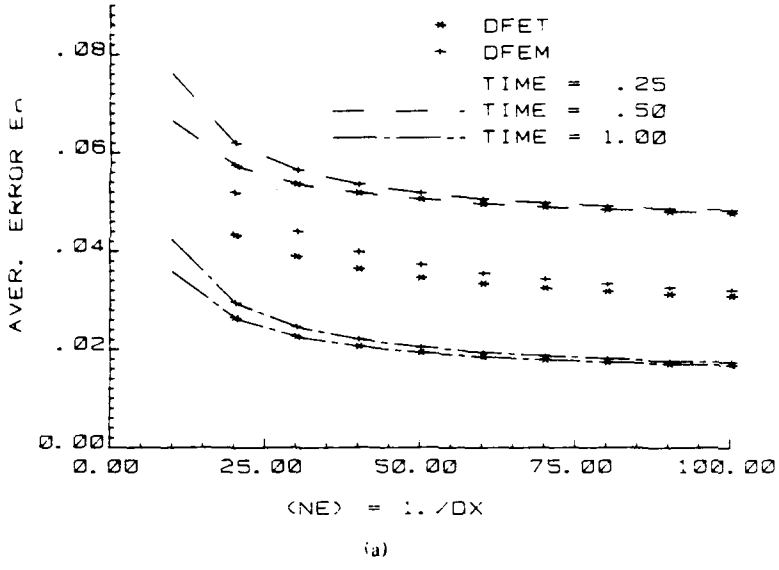

(a)

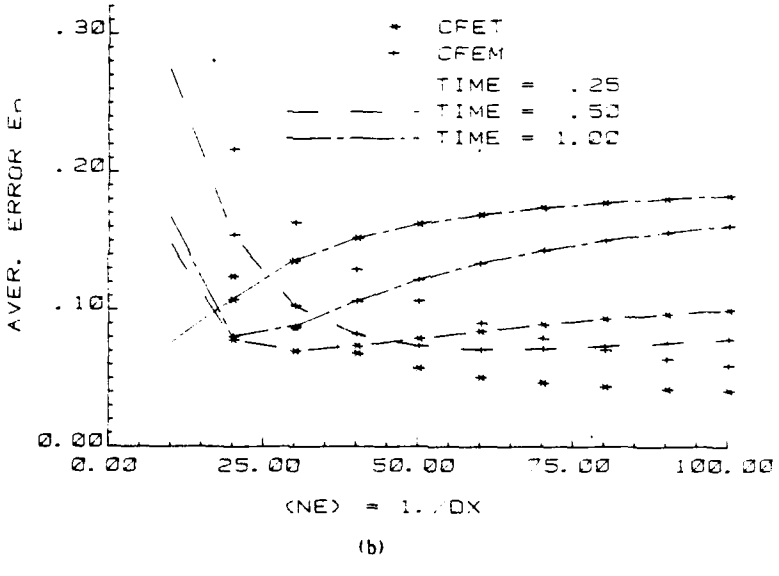

(b)

Fig. 15 — Average error ($V_0 = 0.0$, $D_0 = 1.0$): (a) Displacement models $M_1 = 0.5$ and (b) Conventional models $M_2 = 5.0$

Numerical experimentations based on the average error result not only in a good understanding of the overall behavior of the numerical models but also how the numerical solutions obtained by these models are affected by the parameters M_1 or M_2. From the results presented in the last two sections and from previous studies some optimum values for M_1 and M_2 can be determined. These optimum values should correspond to small error but at the same time should hold the efficiency of the computational model at a high level. The range of values for M_1 is between 0.1 and 0.3 and for M_2 is between 2.0 and 4.00. The exact choice of value sometimes depends on the conditions of the specific problems and one might have to choose a smaller value for M_1 or M_2.

The experience gained from studying the error behavior can be used for obtaining solutions to specific problems. From such solutions one can evaluate the efficiency of a computational model in a more detailed fashion, and with respect to other parameters such as boundary conditions. In the next section several problems will be presented for that purpose.

4.4 Numerical Examples

The computational models developed in this study will be applied to solve the general transport equation for a number of physical problems. Numerical solutions of the transport equation, with the associated boundary conditions are discussed in this section and results obtained from the displacement (DFET) and conventional (CFET) models are compared to available analytical solutions. Results for all case studies were obtained by using $NE = 50$ ($\Delta x = 0.02$) and $M_1 = 0.25$ for the DFET model and $M_2 = 2.5$ for the CFET one. The corresponding time steps are indicated on the figures for each case study.

4.4.1 Advection Equation

This is the simplest form of the general transport equation representing a number of physical processes such as mass conservation, convection of heat and free surface elevation in flow problems.

The typical advection equation is given by

$$\frac{\partial \rho}{\partial t} + V_o \frac{\partial \rho}{\partial x} = 0 \tag{92}$$

for constant velocity fields. Here the transport variable is represented by the dimensionless density ρ. In terms of the displacement field $H(x,t)$ the above equation is expressed as

$$\frac{\partial H}{\partial t} + V_o \frac{\partial H}{\partial x} = 0 \tag{93}$$

with

$$\rho(x,t) = \frac{\partial H(x,t)}{\partial x}. \tag{94}$$

A typical set of initial and boundary conditions for the advection equation are

$$\begin{aligned} &\rho(x,o) = 0.0 \quad 0.0 \leqslant x \leqslant 1.0 \\ &\rho(o,t) = 1.0 \quad t > 0.0. \end{aligned} \tag{95}$$

Numerical solutions are obtained for Eq. (93), displacement models, and for Eq. (92), conventional models. For the displacement model the density ρ is evaluated through the constraint given by Eq. (94) and the same equation is used to express the initial and boundary condition in terms of the displacement field.

The first two figures (16a and b) show results obtained by the two models for the classical problems of a discontinuity advected through space at four different time levels. Both models show the same typical overshoots and the overall error is about the same for both models. No attempt was made to suppress these oscillations since a realistic evaluation of the models is sought. In the second two figures (17a and b) results are given for a different case of the advection equation. A point source term is now included in the equation, with constant rate of production equal to one. The source is placed at $x = 0.5$ and the mass produced is advected to the right with velocity $V_o = 1.0$. For the CFET model some oscillations exist in the region ($x < 0.5$) before the source. There oscillations are much smaller for the DFET model. The oscillatory behavior of the CFET model is due to the discontinuity in the density field imposed by the presence of the source term at $x = 0.5$. At the same point, the displacement field is continuous and has a slope of one according to Eq. (9). The absence of discontinuities in

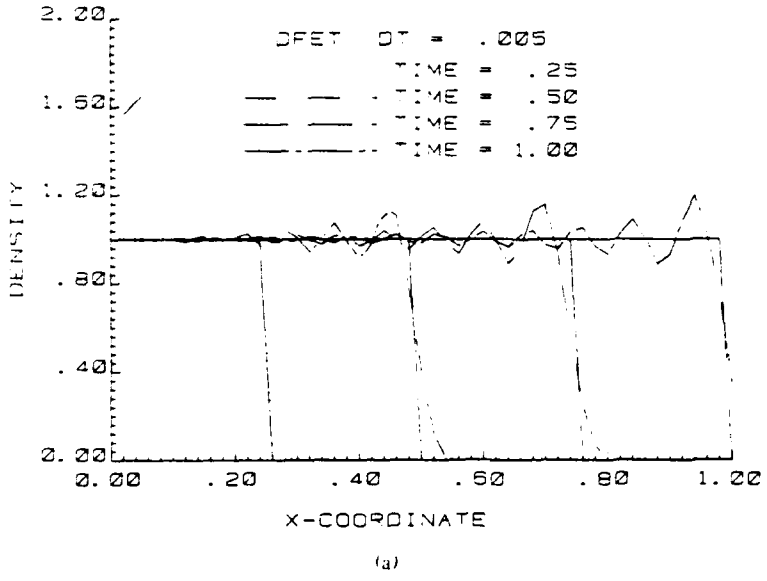

(a)

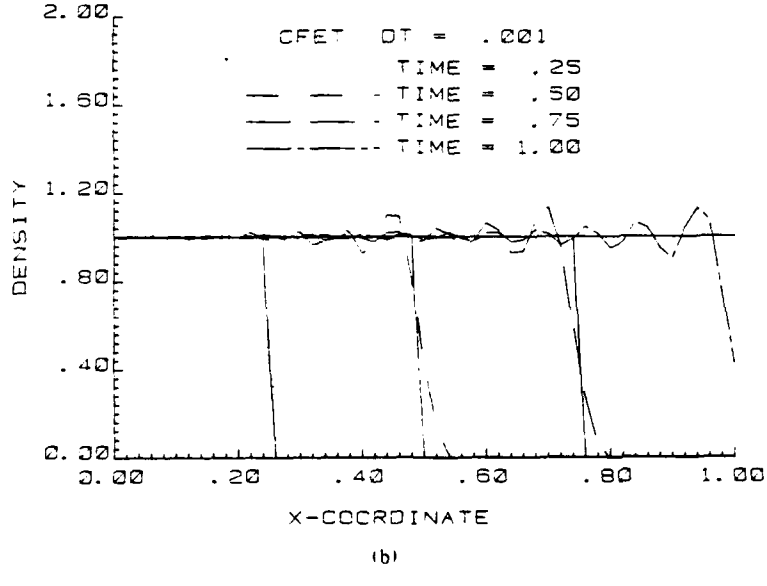

(b)

Fig. 16 — Density distribution ($V_0 = 1.0$, $D_0 = 0.0$): (a) Displacement model and (b) Conventional model

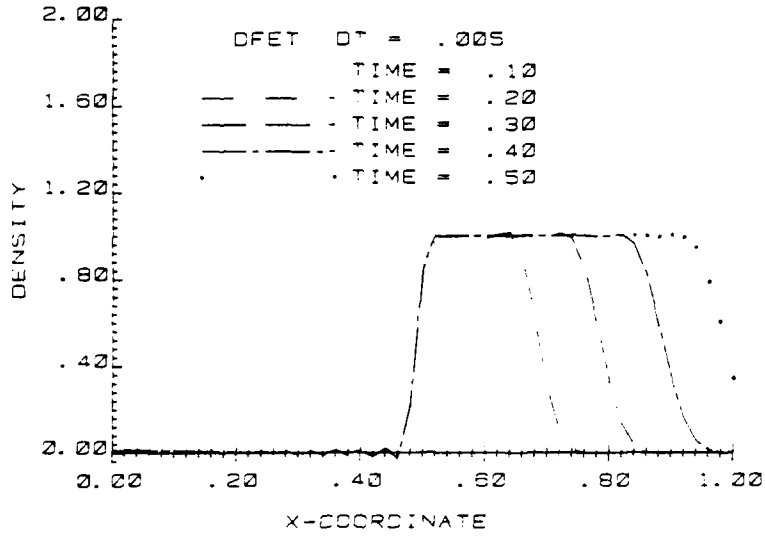

(a)

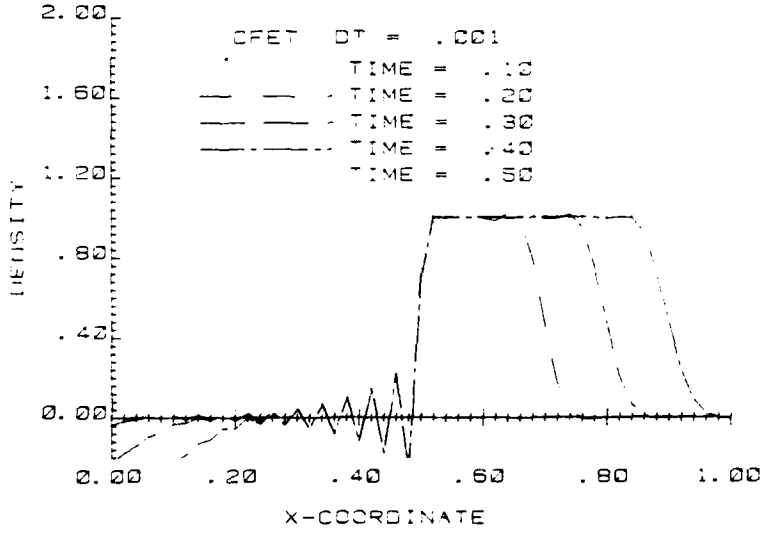

(b)

Fig. 17 — Density distribution ($V_0 = 1.0$, $D_0 = 0.0$): (a) Displacement model and (b) Conventional model

the displacement field not only reduces the oscillations about $x = 0.5$ but also results in a more stable solution, as one can observe from the values of the density, close to the left hand boundary ($x = 0$). Some of the solutions in the next examples show similar behavior and by a closer look at the displacement model one can observe that boundary conditions are better handled when they are imposed through the displacement formulation.

Although the advection equation is the simplest form of partial differential equation, its numerical solution is challenging and a large number of publications exist on other types of initial or boundary conditions as well as different approaches. In the present cases the finite element method, in its simplest form, was applied for the two derived formulations. Since the main objective here is to evaluate the conventional and displacement formulations, we will continue to use linear finite element approximations for all cases of the transport equation.

4.4.2 Convection — Diffusion

The inclusion of a second order space derivative in the advection equation results in the convection-diffusion equation. This is the governing equation for a number of physical processes such as convective heat transfer and energy balance, convective transport of species, pollutants, and momentum transfer. The basic convection-diffusion equation is given by

$$\frac{\partial \Theta}{\partial t} + V_o \frac{\partial \Theta}{\partial t} - D_o \frac{\partial^2 \Theta}{\partial x^2} = 0 \tag{97}$$

for a constant velocity field and diffusivity.

Here the transport variable is represented by the dimensionless temperature $\Theta(x,t)$ which relates to the transport (heat) displacement in the same fashion as for the density

$$\Theta(x,t) = \frac{\partial H(x,t)}{\partial x} \tag{98}$$

If a source term and a heat transfer term are included in the convection-diffusion equation, then Eq. (97) is written as

$$\frac{\partial \Theta}{\partial t} + V_o \frac{\partial \Theta}{\partial x} - D_o \frac{\partial^2 \Theta}{\partial x^2} = S_o S - K_o \Theta \tag{99}$$

where S_o is the coefficient associated with the heat source term S ($S_o = 0$ or 1) and K_o is the heat transfer coefficient.

In terms of the heat displacement field $H(x,t)$ the convection-diffusion equation is written as

$$\frac{\partial H}{\partial t} + V_o \frac{\partial H}{\partial x} - D_o \frac{\partial^2 H}{\partial x^2} = S_o \dot{h} - K_o H \tag{100}$$

Initial and boundary conditions associated with this equation are numerous. Here some typical boundary conditions are considered and numerical solutions will be obtained for both computational models. In Table 10 the initial and boundary conditions are given for each of the problems considered.

Table 10

Problem	V_o	D_o	S_o	K_o	Initial Conditions	Boundary Conditions $L \rightarrow \infty$	Figures
1	1.0	1.0	0.0	0.0	$\Theta(x,0) = 0.0$	$\Theta(1,0) = 1.0, \Theta(L,0) = 0.0$	18
2	1.0	1.0	0.0	0.0	$\Theta(x,0) = 0.0$	$\Theta(1,0) = \sin \omega t, \Theta(L,0) = 0.0$	19
3	1.0	1.0	1.0	0.0	$\Theta(x,0) = 0.0$	$\Theta(0,t) = 0.0, \Theta(L,0) = 0.0$	20
4	1.0	1.0	1.0	0.0	$\Theta(x,0) = 0.0$	$\frac{\partial \Theta}{\partial x}(0,t) = 0.0, \Theta(L,0) = 0.0$	21
5	1.0	1.0	1.0	0.0	$\Theta(x,0 = 0.0$	$\Theta(-L,t) = 0.0, \Theta(L,t) = 0.0$	22
6	1.0	1.0	1.0	1.0	$\Theta(x,0) = 0.0$	$\Theta(0,t) = 0.0, \Theta(L,0) = 0.0$	23

In the first problem the right hand side boundary condition ($x = L$) is assumed to be applied at infinity. This condition will be assumed in all problems considered in the following examples. For the heat source term the value of S_o is 1.0 at $x = 0.5$ and 0.0 elsewhere with $\dot{h}(0.5,t) = 1.0$ This represents a point heat source at $x = 0.5$ with unit heat generation per unit time. Numerical results for the problems described in Table 10 are given in Figs. 18 through 23.

The first problem is the typical case for the convection-diffusion equation for a constant temperature applied on the left hand side boundary. The physical boundary to the right is at infinity and the computational boundary is at $x = 1.0$. Since the boundary condition $\Theta(L,t) = 0.0$, is at infinity, then it is physically incorrect to apply this boundary condition at $x = 1.0$. The temperature at $x = 1.0$ is zero for small times ($t < 1.0$) but it is not zero for larger times. Therefore no boundary condition is imposed at $x = 1.0$ and the computational model should be able to simulate an outflow boundary at that point.

In Fig. 18a results for the DFET model are given for four time intervals and the numerical solution is compared to the analytical one (solid lines). The agreement between the two is good and the largest error occurs close to the right hand side boundary. Similar results are given in Fig. 18b for the CFET model for the temperature distribution. The error of the CFET model is larger than the DFET one throughout the computational domain. The larger error occurs mainly because of the error introduced by the boundary conditions. The boundary forces resulting from the variational formulation are given by

$$Q_i = \int_s \eta \frac{\partial \Theta}{\partial x} \frac{\partial \Theta}{\partial q_i} ds \tag{101}$$

for the CFET model, and

$$Q_i = \int_s \eta \Theta \frac{\partial H}{\partial q_i} ds \tag{102}$$

for the DFET model.

If a boundary condition is described for the temperature at $x = 0.0$ ($\Theta(0,t) = 1.0$) then

$$\delta\Theta = 0 \rightarrow \frac{\partial \Theta}{\partial q_i} = 0$$

which means that the boundary force at $x = 0.0$ is zero for the CFET model. This is not the case for the DFET model since δH_i is not zero. At the other boundary ($x = 1.0$) the same is true for both models if the temperature is described at that boundary. As was mentioned before no boundary condition is imposed at $x = 1.0$, which means that the boundary forces are not zero and should be included in the calculation for both models. By retaining the boundary forces the results for the DFET model, Fig. 18a, show a good agreement with the analytical solution and the boundary force accounts for the neglected portion of the physical domain ($x > 1$). The inclusion of the boundary force in the computations for the DFET model is also in agreement with the theory since neither $\Theta(1,t)$ nor δH_i is zero.

Although theory and results are in agreement for the displacement formulation the same is not true for the conventional one. If one retains the boundary force in the computations, the results, given in Fig. 18c, show very large error close to the boundary ($x = 1.0$) but if the boundary force is set equal to zero, even though Θ or $\delta\Theta$ are not zero, then the results, given in Fig. 18b, show much less error

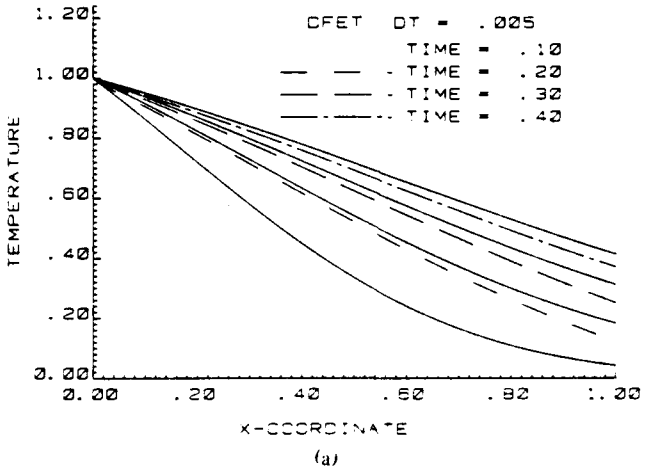

(a)

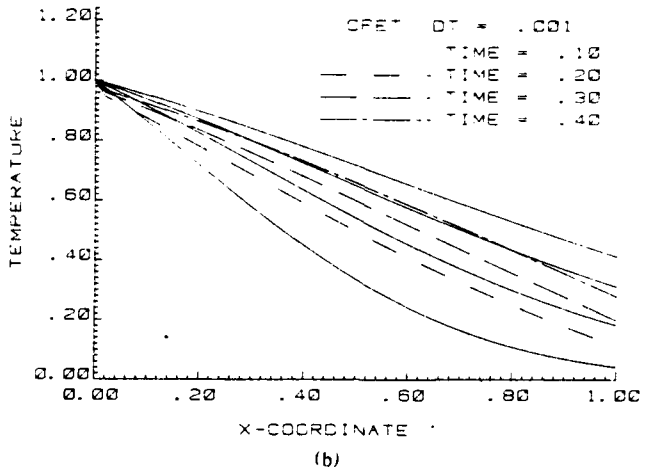

(b)

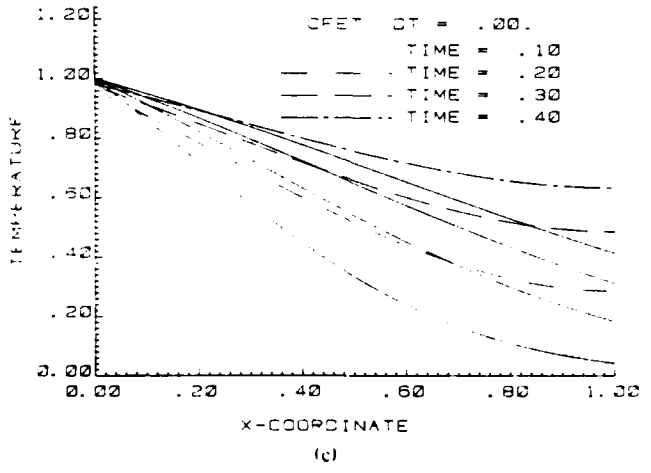

(c)

Fig. 18 — Temperature distribution ($V_0 = 1.0$, $D_0 = 1.0$, Problem 1): (a) Displacement model, (b) Conventional model and (c) Conventional model with boundary forces

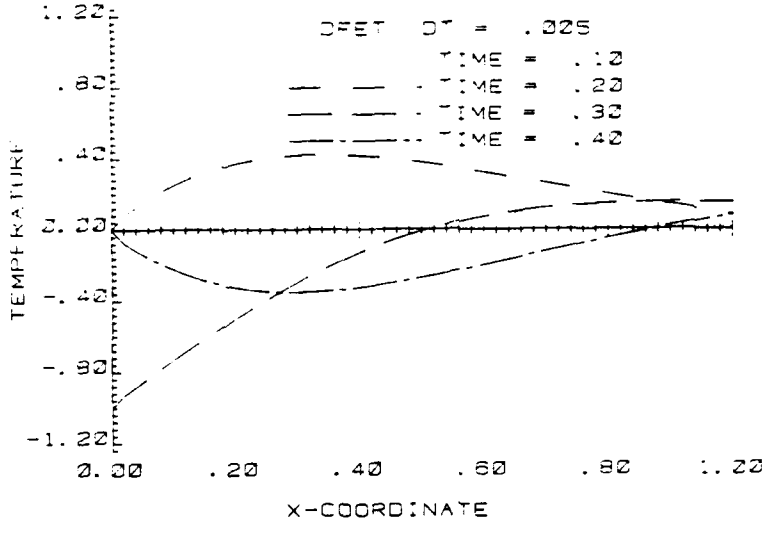

(a)

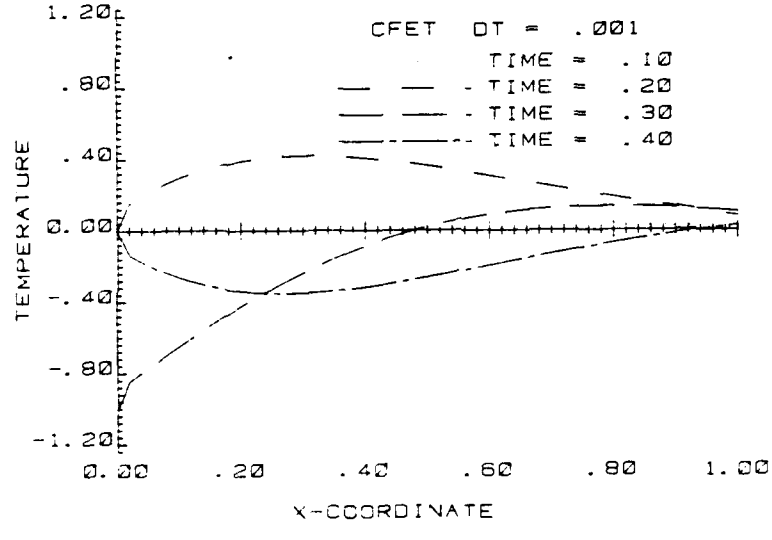

(b)

Fig. 19 — Temperature distribution ($V_0 = 1.0$, $D_0 = 1.0$, Problem 2): (a) Displacement model and (b) Conventional model

and the temperature distribution is similar to the DFET model. This discrepancy in the results obtained by the CFET model exists in all cases of solving problems in the semi-infinite space. There is a deficiency of the conventional formulation in terms of properly simulating outflow conditions. For all these types of problems even if the boundary conditions are not explicitly imposed, the boundary forces should be zero for the CFET model. This is in agreement with the Galerkin approach and the term "consistent model" will be used for the CFET model with no boundary forces. For the second problem, where a sinusoidal wave ($\omega = \pi/.2$) is applied at the boundary ($x = 0$), results are presented in Figs. 19a and 19b for each of the two models. A comparison of these two figures shows a good arguement between the two models but it should be noted that the results for the CFET model were obtained by using a time step five times smaller than the one used for the DFET model. This is the case for all the results obtained in this study, where in order to achieve results of about the same accuracy the CFET model requires a time step five times smaller.

The next example, problem 3, is the case when a point heat source is present at $x = 0.5$. Results for the DFET model are given in Fig. 20a and for the CFET model in Figs. 20b and 20c. In the last two figures results are given for cases of omission and inclusion of the boundary force ($x = 1.0$) respectively as previously for problem 1. As one can observe from Fig. 20b (no boundary force) the results for the consistent model are in good agreement with the ones of the DFET model, Fig. 20a. But when the boundary force is included, Fig. 20c, the temperature distribution results in much larger values close to the boundary ($x = 1.0$). This behavior of the CFET model is the same as previously in problem 1. For the rest of the problems in this section the results for the CFET model are with no boundary force. In problem 4 a point heat source is present, as in the previous problem, and the boundary conditions are of no flow of heat at the left boundary and zero temperature at infinity. The results for the two models are presented in Fig. 21a and 21b. The temperature distribution shows good agreement at the left boundary but again at the outflow boundary the temperature is lower for the CFET model. This has been the case for all three previous examples. If one now considers a infinite domain and that the temperature is zero at $-L$ and $+L$ ($L \rightarrow \infty$), the heat generated by a point heat source will be convected to the right and diffused in both directions according to the governing equation.

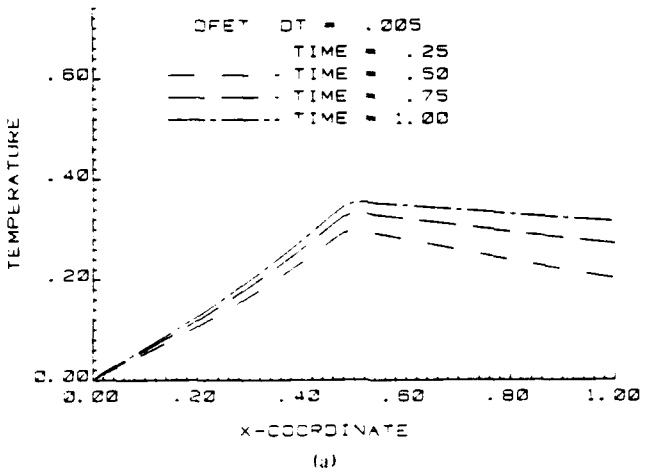

(a)

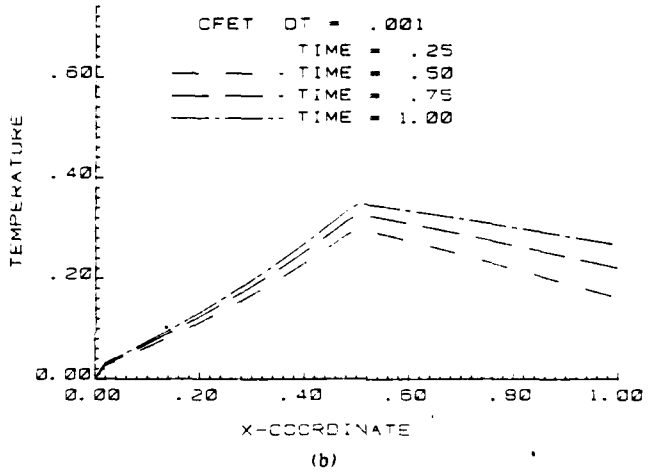

(b)

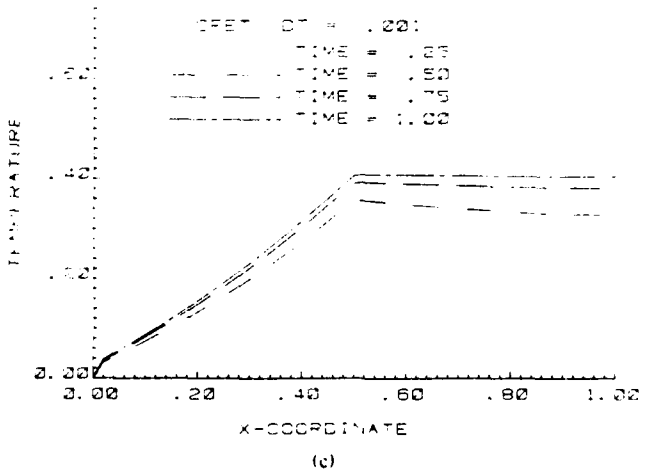

(c)

Fig. 20 — Temperature distribution ($V_0 = 1.0$, $D_0 = 1.0$, Problem 3): (a) Displacement model, (b) Conventional model and (c) Conventional model with boundary forces

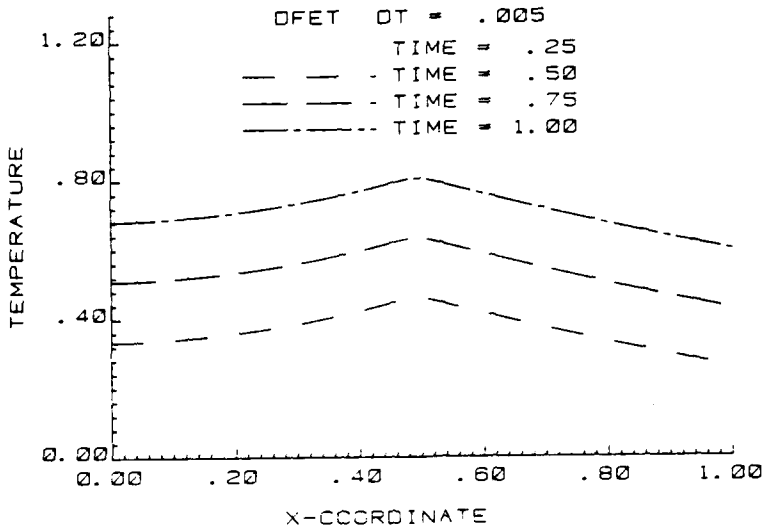

(a)

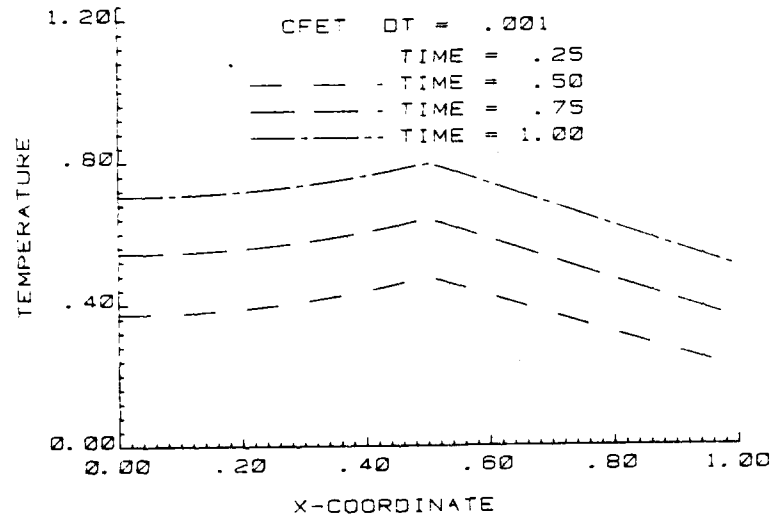

(b)

Fig. 21 — Temperature distribution ($V_0 = 1.0$, $D_0 = 1.0$, Problem 4): (a) Displacement model and (b) Conventional model

Numerical results for the solution of this problem are given in Fig. 22a and 22b for the two models. The temperature distribution obtained from the CFET model is almost twice as high than the one obtained in the DFET model at the left side of the computational boundary and it is lower to the right of the heat source. Again this is due to the way that outflow boundary conditions are simulated by the CFET model. As a last example for the convection and diffusion of heat a case is presented, problem 5, where heat is lost throughout the space ($(0 \leqslant x < \infty)$) due to the heat transfer term in the governing equation. Results for this case are given in Fig. 23a and 23b for the two models. These two figures should be compared with Figs. 20a and 20b where results are given for the same problem but with no heat loss. As it is expected the temperature distribution for problem 5 is lower than the one for problem 3 throughout the computational domain.

For all case studies considered here both computational models give good results for problems where the boundary conditions are well defined. On the other hand when the outflow conditions exist, the CFET model yields results at that boundary which are always lower to the corresponding results of the DFET model. Furthermore, for such cases where analytical solutions are available, a comparison with the numerical solutions shows that the CFET model yields always a lower distribution than the DFET model.

The failure of the CFET model to simulate correctly outflow conditions is related mainly to the fact that the conventional model cannot account for the presence of the physical space beyond the computational one. This deficiency results in more heat flowing out at the end of the computational boundary, thus lower temperature distributions. In the next section similar behavior is observed for the diffusion of heat in the half space.

4.4.3 Diffusion Equation

In the case of a solid medium or a fluid not in motion the convective term of the transport equation is zero and the governing equation is given by

$$\frac{\partial \Theta}{\partial t} - D_0 \frac{\partial^2 \Theta}{\partial x^2} = 0 \tag{103}$$

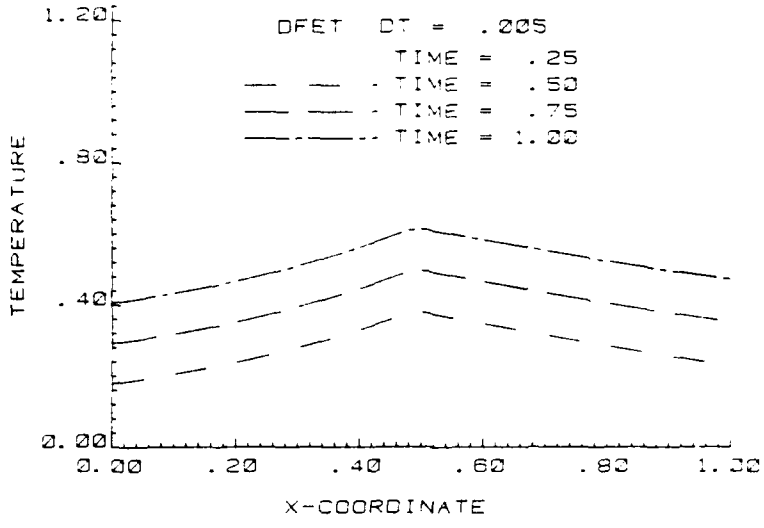

(a)

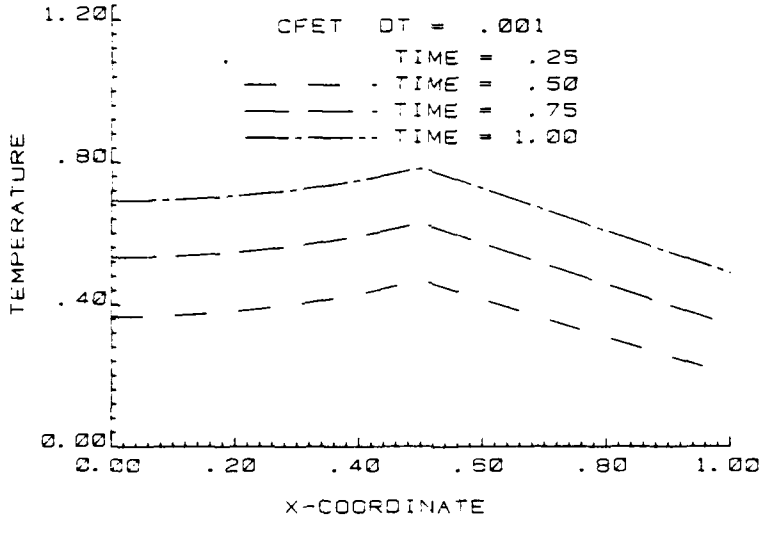

(b)

Fig. 22 — Temperature distribution ($V_0 = 1.0$, $D_0 = 1.0$, Problem 5): (a) Displacement model and (b) Conventional model

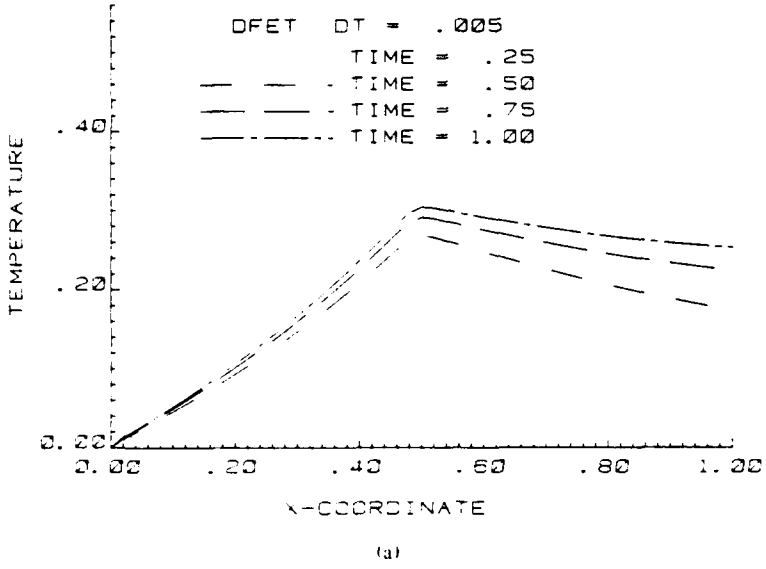

(a)

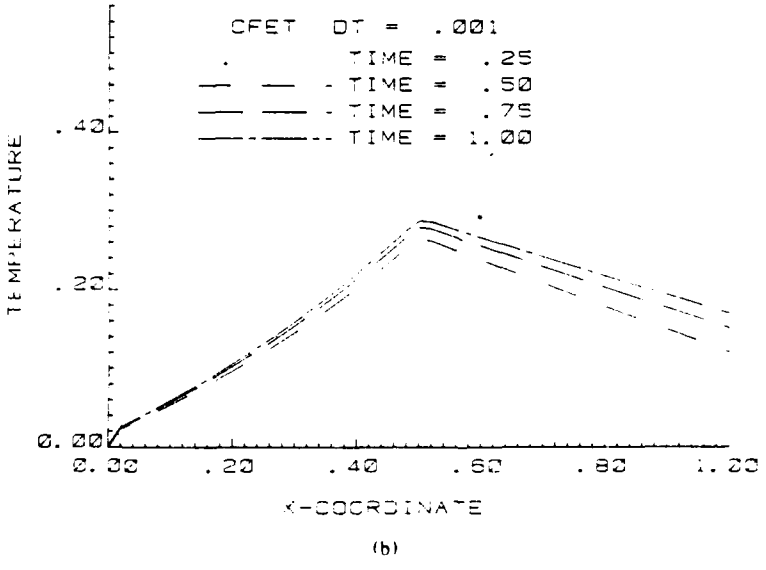

(b)

Fig. 23 — Temperature distribution ($V_0 = 1.0$, $D_0 = 1.0$, Problem 6): (a) Displacement model and (b) Conventional model

with $\Theta(x,t)$ the dimensionless temperature which is related to the heat displacement $H(x,t)$ by Eq. (98).

Table 11

Problem	D_o	S_o	K_o	Initial Conditions	Boundary Conditions	Figure
1	1.0	0.0	0.0	$\Theta(x,0) = 0.0$	$\Theta(0,t) = 1.0$ $\Theta(L,t) = 0.0$	24
2	1.0	0.0	0.0	$\Theta(x,0) = 0.0$	$\Theta(0,t) = \sin(\omega t)$ $\Theta(L,t) = 0.0$	25
3	1.0	1.0	0.0	$\Theta(x,0) = 0.0$	$\Theta(0,t) = 0.0$ $\Theta(L,t) = 0.0$	26
4	1.0	1.0	0.0	$\Theta(x,0) = 0.0$	$\Theta(-L,t) = 0.0$ $\Theta(L,t) = 0.0$	27
5	1.0	0.0	0.0	$\Theta(x,0) = 0.0$	$\Theta(0,t) = 1.0$ $\Theta(1,t) = 0.0$	28
6	1.0	0.0	0.0	$\Theta(x,0) = 0.0$	$\Theta(0,t) = 1.0$ $\frac{\partial \Theta}{\partial x}(1,t) = 0.0$	29
7	1.0	0.0	0.0	$\Theta(x,0) = 0.0$	$\Theta(0,t) = 1.0$ $\frac{\partial \Theta}{\partial x}(1,t) = \Theta(1,t)$	30
8	1.0	1.0	0.0	$\Theta(x,0) = 0.0$	$\Theta(0,t) = 0.0$ $\Theta(1,t) = 0.0$	31
9	1.0	1.0	0.0	$\Theta(x,0) = 0.0$	$\frac{\partial \Theta(0,t)}{\partial x} = 0.0$ $\frac{\partial \Theta(1,t)}{\partial x} = 0.0$	32
10	1.0	1.0	1.0	$\Theta(x,0) = 0.0$	$\frac{\partial \Theta(0,t)}{\partial x} = 0.0$ $\frac{\partial \Theta(1,t)}{\partial x} = 0.0$	33

The initial and boundary conditions associated with Eq. (103), for the case studies considered here, are given in Table 11. The first four problems are for the diffusion of heat in the semi-infinite space ($L \rightarrow \infty$) and the last six for problems of finite space ($0.0 \leqslant x < 1.0$) . The first problem is the classical case of constant temperature at $x = 0.0$ and zero temperature at infinity. Results are given in Figs. 24a and 24b, for the two models, and they are compared to the analytical solution (solid line). As was previously observed, for the case of convection-diffusion, the temperature distribution for the CFET model is lower than the DFET model. The error in the results of the CFET model is larger for the diffusion case than for the convection diffusion one. This should be expected since the diffusion term is the dominent term in the present case, thus the boundary force plays a more important role in simulating outflow conditions. Similar observations can be made for the third and fourth problems,

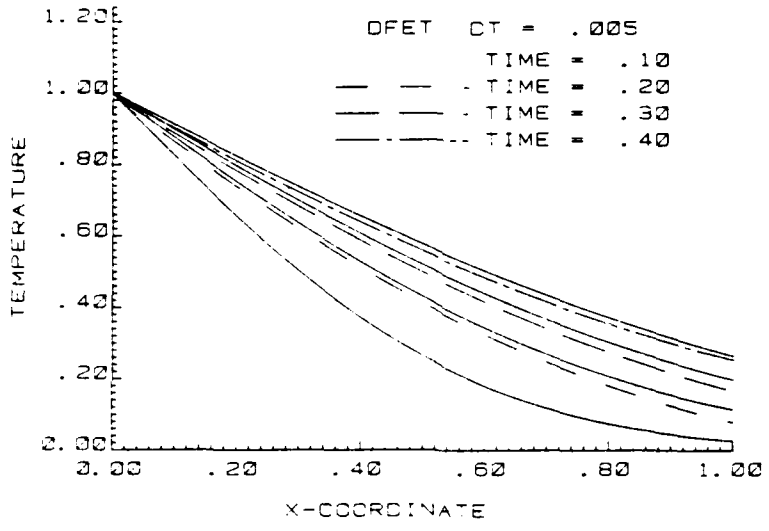

(a)

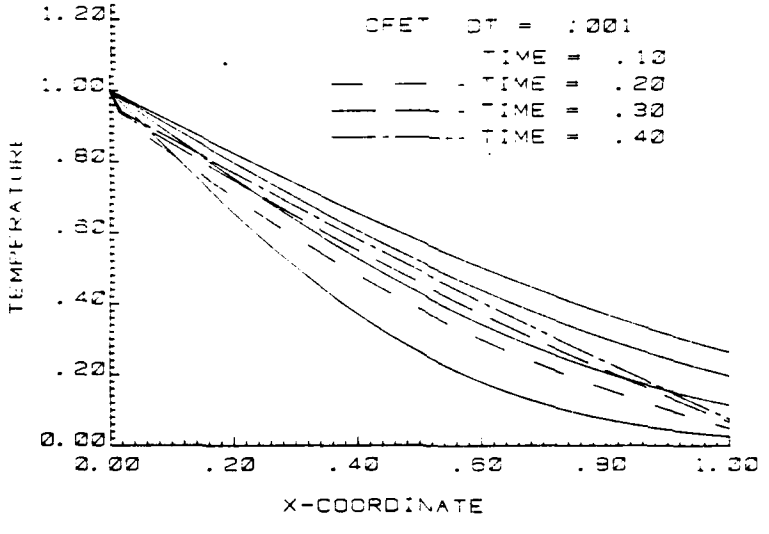

(b)

Fig. 24 — Temperature distribution ($V_0 = 0.0$, $D_0 = 1.0$, Problem 1): (a) Displacement model and (b) Conventional model

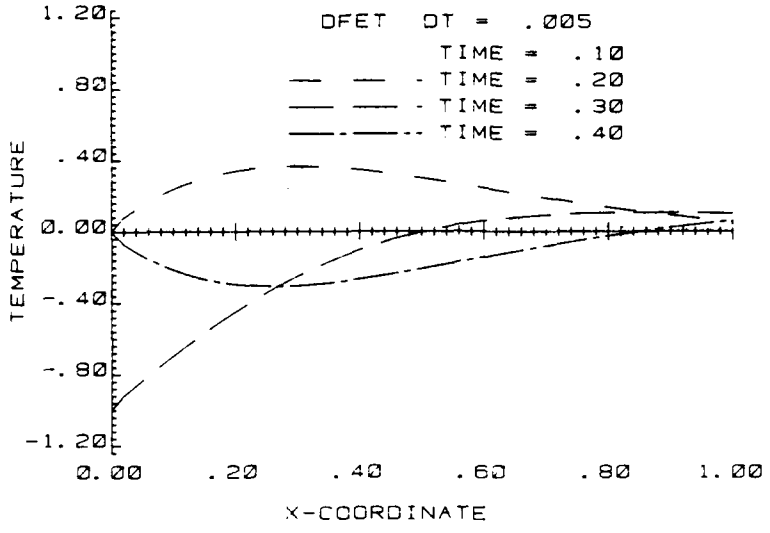

(a)

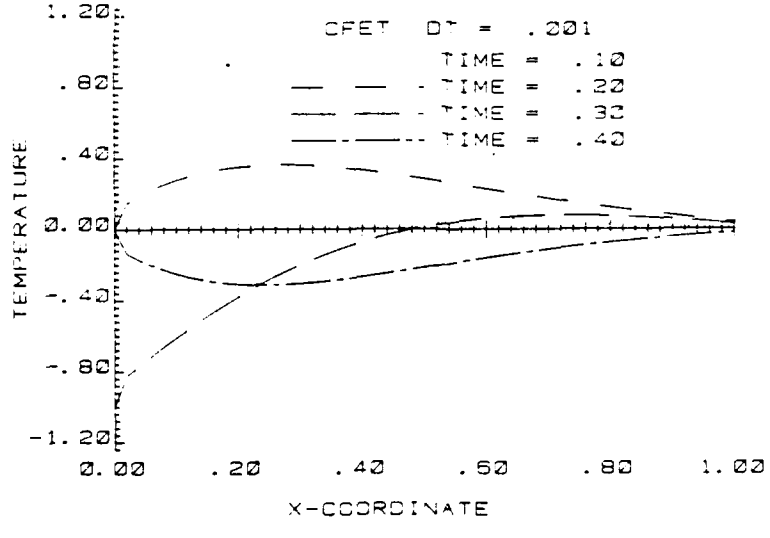

(b)

Fig. 25 — Temperature distribution ($V_0 = 0.0$, $D_0 = 1.0$, Problem 2): (a) Displacement model and (b) Conventional model

Figs. 26 and Figs. 27. For both problems a point heat source is located at $x = 0.5$ and the boundary conditions are given in Table 11. For problem 3 a comparison of results between the DFET model, Fig. 26a and the consistent CFET model (no boundary force at x = 1.0), Fig. 26b, shows a much lower temperature distribution to the right of the heat source. The opposite is true for the results of the CFET model of Fig. 26c.

In the next problem where the computational domain represents an infinite physical domain the temperature distribution should be symmetric with respect to the point heat source. This is true for the results of the DFET model, Fig. 27a, and the results of the CFET model when the boundary forces are included, Fig. 27c but it is not true for the results obtained by the consistant CFET model. Throughout the results presented in the previous and present sections an important difference exists between the two models. The implementation of the DFET model to solve problems with unbounded domains results in computational models where no inconsistancies exist between the physical and mathematical aspects of the problem. Although this is the case for the DFET model, it is not true for the CFET model where the absence of the boundary forces result in a better numerical solution but the physical and mathematical aspects of the problem contradict each other.

In the last part of this section the diffusion of heat is considered for a finite domain, a slab of thickness one, and the boundary condition for the different cases are given in Table 11. In all examples, problems 5 - 10, the numerical results of the two models are of about the same accuracy. For the finite domain problems, the boundary conditions are applied on both boundaries. The boundary forces are zero for the CFFT model (all examples) but for the DFET model the boundary forces are zero only if the specified boundary temperature is zero. Otherwise the values of the boundary forces depend on the values of the temperature at each boundary.

The numerical results of problems 5 through 10 are presented in Figs. 28 through 33 for the two models. Comparing the results obtained by the two models one can easily observe that the numerical solutions are almost identical. The only difference is that the results of the CFET model were obtained

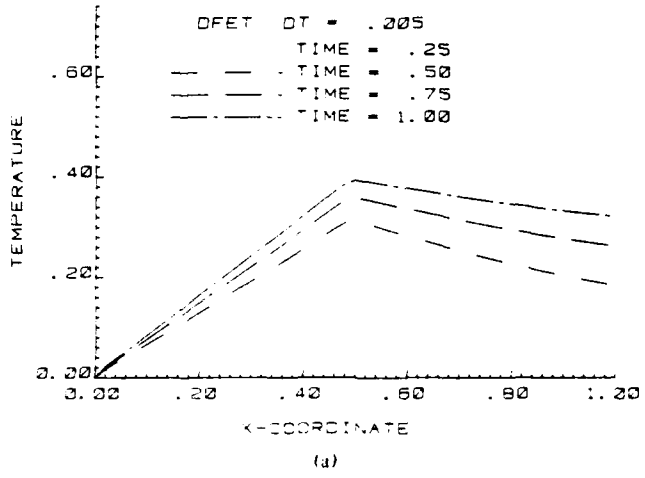

(a)

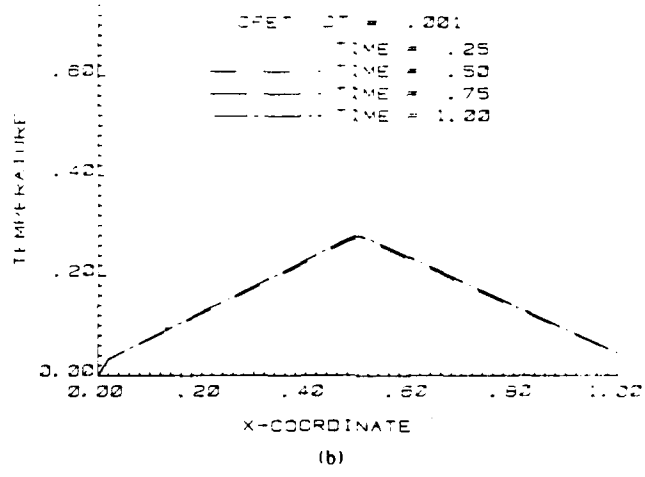

(b)

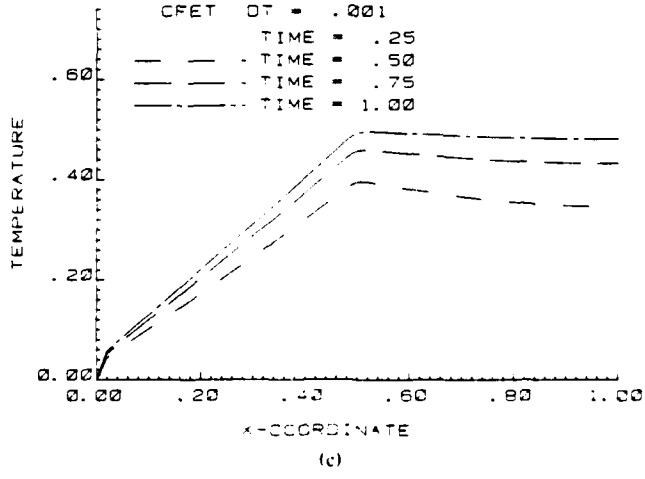

(c)

Fig. 26 — Temperature distribution ($V_0 = 0.0$, $D_0 = 1.0$, Problem 3): (a) Displacement model, (b) Conventional model and (c) Conventional model with boundary forces

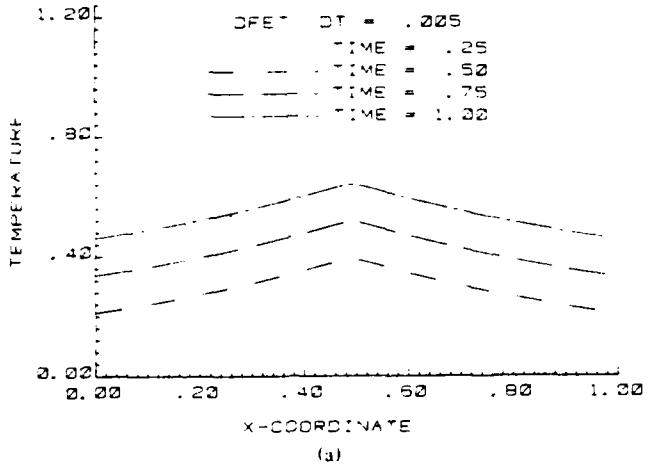

(a)

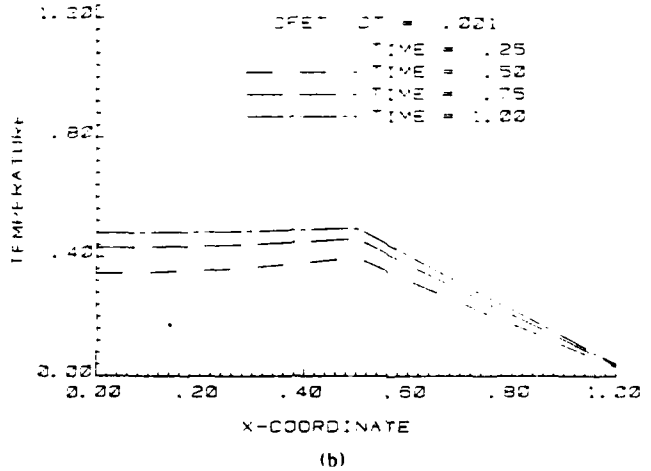

(b)

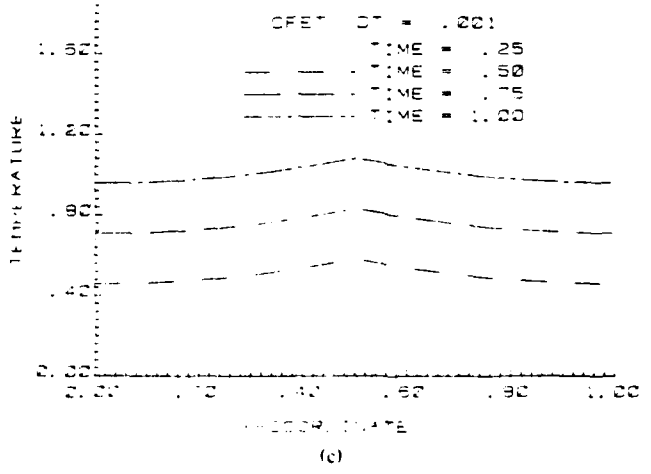

(c)

Fig. 27 — Temperature distribution ($V_0 = 0.0$, $D_0 = 1.0$, Problem 4): (a) Displacement model, (b) Conventional model and (c) Conventional model with boundary forces

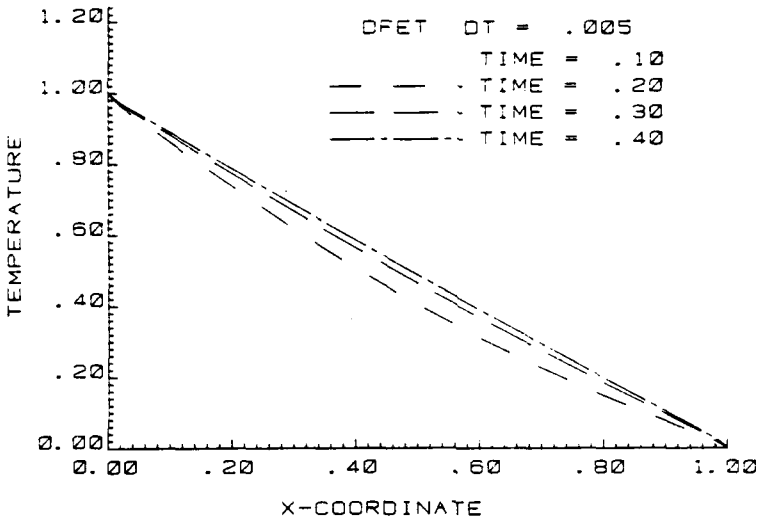

(a)

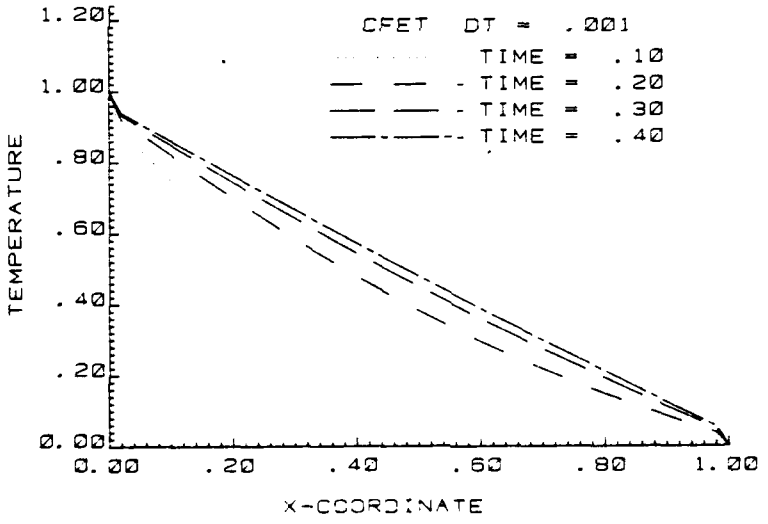

(b)

Fig. 28 — Temperature distribution ($V_0 = 0.0$, $D_0 = 1.0$, Problem 5): (a) Displacement model and (b) Conventional model

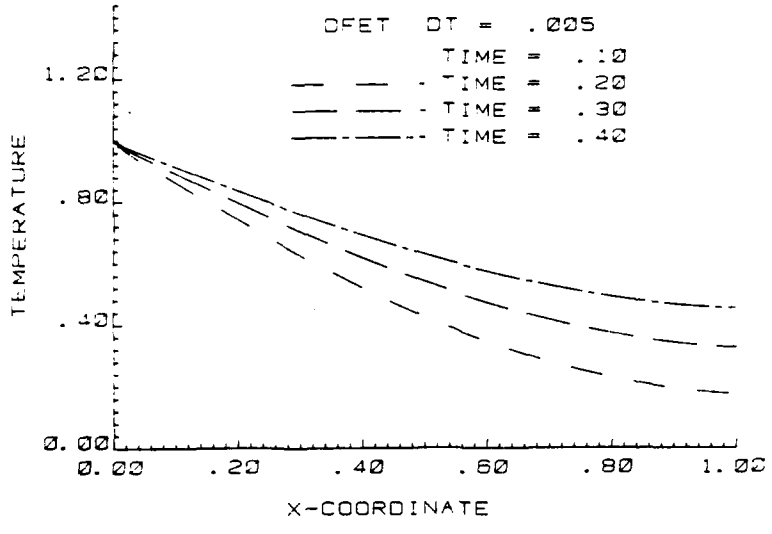

(a)

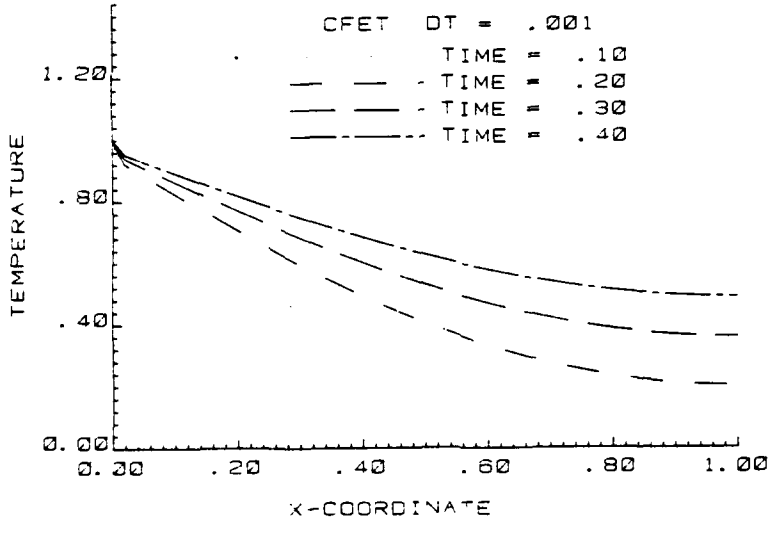

(b)

Fig. 29 — Temperature distribution ($V_0 = 0.0$, $D_0 = 1.0$, Problem 6): (a) Displacement model and (b) Conventional model

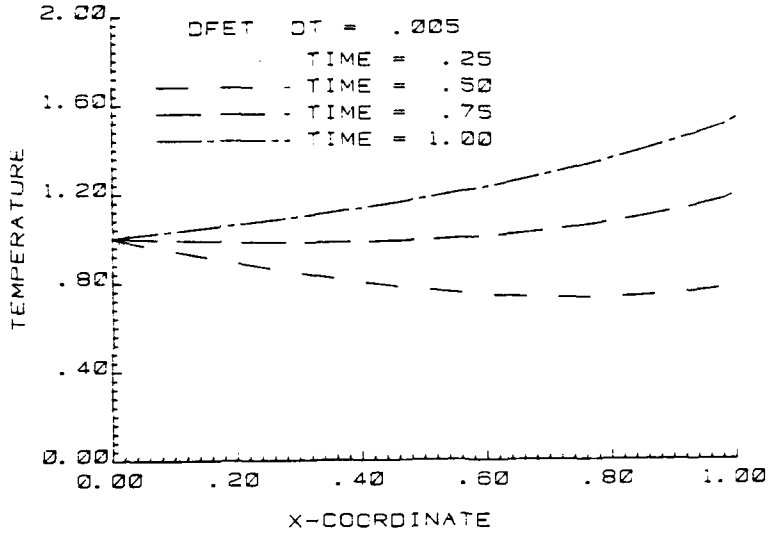

(a)

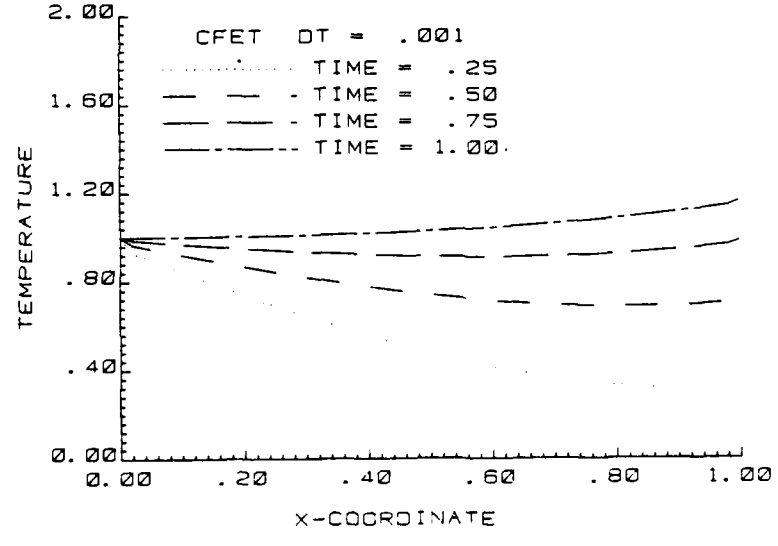

(b)

Fig. 30 — Temperature distribution ($V_0 = 0.0$, $D_0 = 1.0$, Problem 7): (a) Displacement model and (b) Conventional model

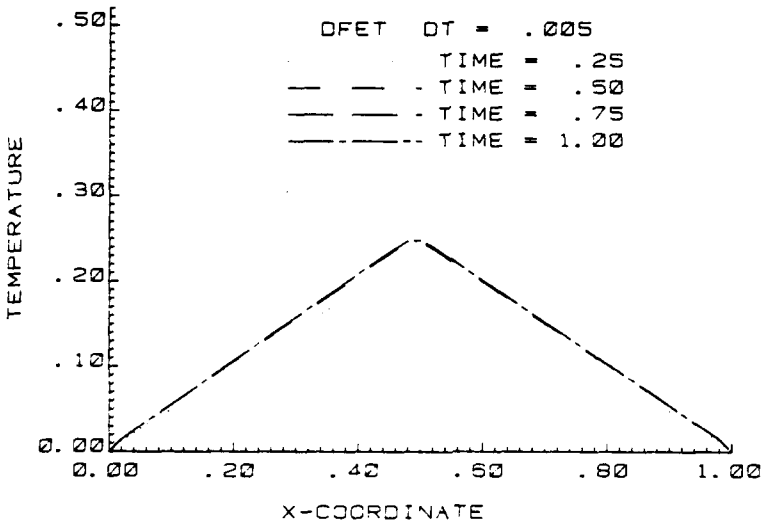

(a)

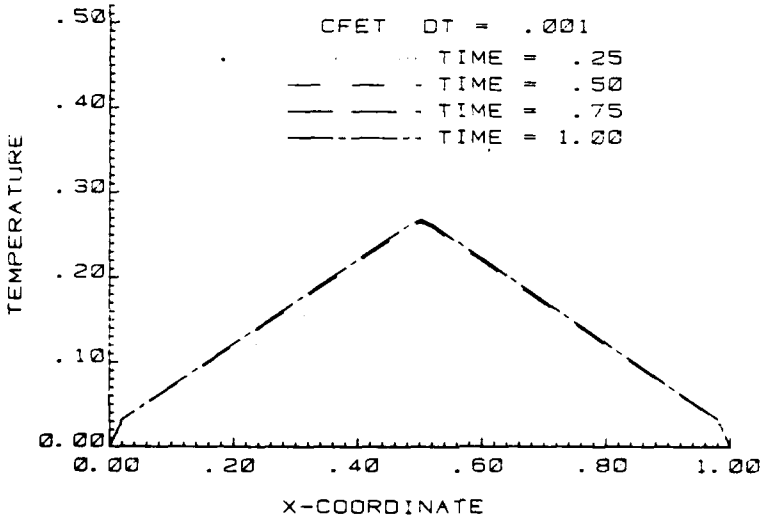

(b)

Fig. 31 — Temperature distribution ($V_0 = 0.0$, $D_0 = 1.0$, Problem 8): (a) Displacement model and (b) Conventional model

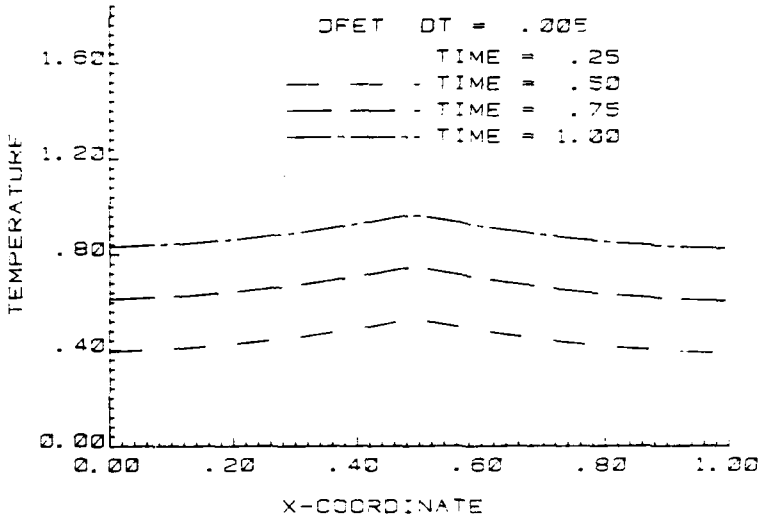

(a)

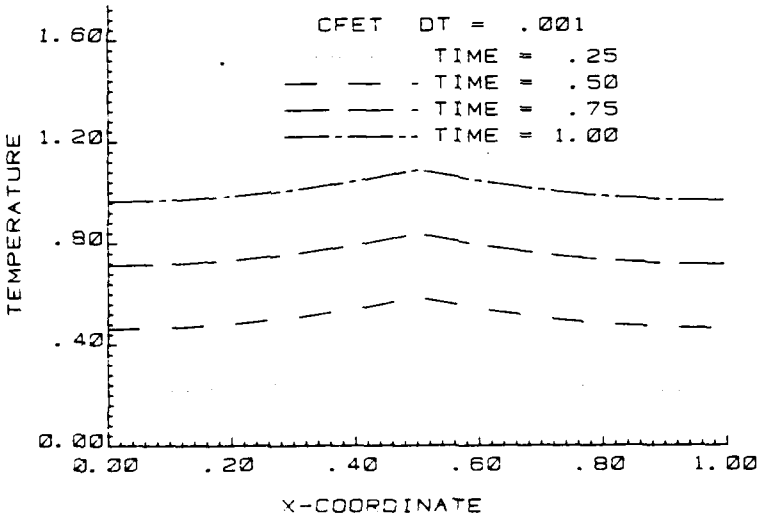

(b)

Fig. 32 — Temperature distribution ($V_0 = 0.0$, $D_0 = 1.0$, Problem 9): (a) Displacement model and (b) Conventional model

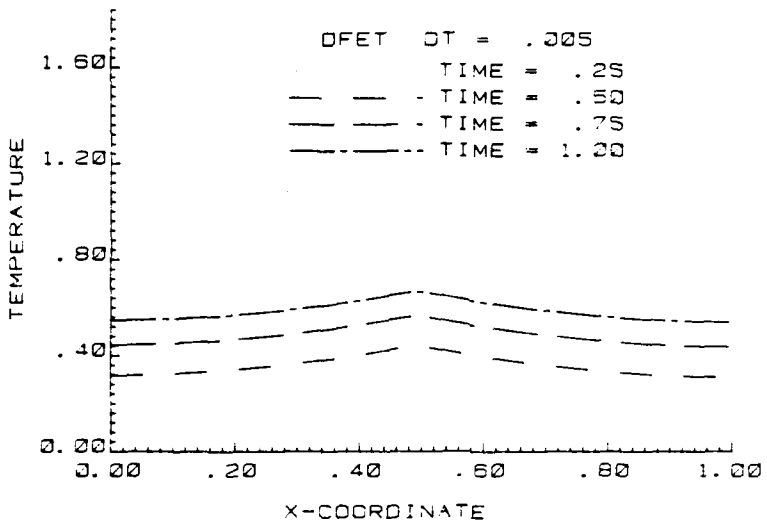

(a)

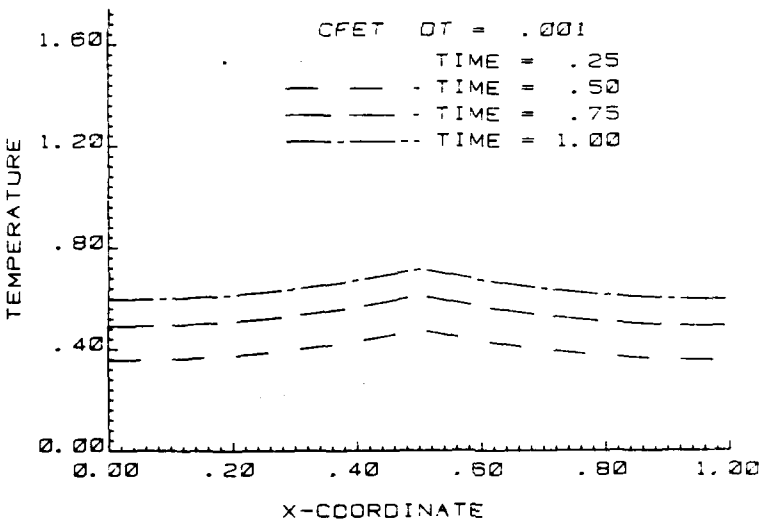

(b)

Fig. 33 — Temperature distribution ($V_0 = 0.0$, $D_0 = 1.0$, Problem 10): (a) Displacement model and (b) Conventional model

by using a time step size five times smaller than the one used for the DFET model. Therefore from the computational point of view the displacement formulation is more efficient since it requires less time to solve a problem. If the problem to be solved does not have outflow boundary conditions, both models produce numerical solutions of the same accuracy.

Throughout the examples presented here one can observe the displacement formulation, the DFET model, is more consistent than the conventional one with respect to handling different physical problems. This is justified not only from the numerical solutions obtained but also from the formulation on which the displacement model is based.

SUMMARY AND CONCLUSIONS

A variational formulation for the transport equation has been presented in this study, and, based on this formulation, a generalized approach to approximate solutions has been developed. As a special application to approximate solutions four computational models were derived for obtaining numerical solutions to different types of transport problems. The models are based on first-order finite element approximations for both the spatial and time coordinates. Two of the models are derived from the fundamental variational analysis in terms of the transport displacement and the other two are derived from the complementary variational analysis in terms of primitive transport variable. Although only linear and one-dimensional models were considered here, higher order and multi-dimensional models can be easily obtained since the derived formulation is not restricted to one type of approximation or one dimension.

An evaluation of the four computational models with respect to accuracy and efficiency was carried out, first, by numerical experimentation on the error behavior and, second, by obtaining numerical solutions to specific boundary value problems.

The investigation of the error of the numerical solution shows that the displacement models not only are more consistent in the error behavior than the conventional ones, but also that the overall

error of the numerical solutions, obtained by the displacement models, is always smaller than the error of the solutions obtained by the conventional ones. The larger error of the conventional models is partially because they are derived from the complementary variational principle, which according to the theory is less accurate than the corresponding fundamental variational principle. Numerical solutions to heat transport problems obtained here also justify this argument. Furthermore, these solutions showed the inability of the conventional models to correctly simulate outflow boundary conditions.

Although the two types of computational models have some common characteristics in behavior, the conventional ones are less efficient from both accuracy and computational effort points of view. Displacement models have been used widely in structures, but as it has been shown these models can be extended to other types of problems as well. Furthermore, the fundamental form of the variational analysis can be derived, based on concepts of classical mechanics presented here, for many governing equations.

In conclusion, the generalized variational analysis and the unified approach in obtaining approximate solutions should be emphasized as well as the applicability of the analysis to other physical problems. It should be also noted that the finite element method, which was presented in this study, is only one restricted application of the generalized formulation.

ACKNOWLEDGEMENTS

This work was partially supported by the research program in Computational Hydrodynamics at the Naval Research Laboratory. The author wishes to thank R. A. Skop and O. Griffin for their valued suggestions.

REFERENCES

1. Biot, M.A., "Thermodynamics and Heat-Flow Analysis by Lagrangian Methods," *Proc. of the 7th Anglo-American Aeronautical Conference*, Inst. of Aero-Sciences, N.Y., 1959, p. 418.

2. Biot, M.A., "New Methods in Heat Flow Analysis with Applications to Flight Structures," *Journal of the Aero. Sciences*, Vol. 24 (12), 1957, p. 857.

3. Keramidas, G.A., "Finite Element Modeling for Convection-Diffusion Problems," NRL Memorandum Report 4225, 1980.

4. Keramidas, G.A., "Finite Element Modeling of the Coupled Thermal and Momentum Diffusion Equations," NRL Memorandum Report 4310, 1980.

5. Biot, M.A., "Variational Principles in Irreversible Thermodynamics with Application to Viscoelasticity," *Phys. Rev.* 97, 1463-1469 (1955).

6. Barger, V.D., Olsson, M., "Classical Mechanics, A Modern Perspective," McGraw-Hill, 1973.

7. Carnahan, B., Luther, H.A., Wilkes, J.O., "Applied Numerical Methods," Clarendon Press, Oxford (1959).

8. Gay, B., Cameron, P.T., "The Efficiency of Numerical Solutions of the Heat Conduction Equation," ASME, 1967.

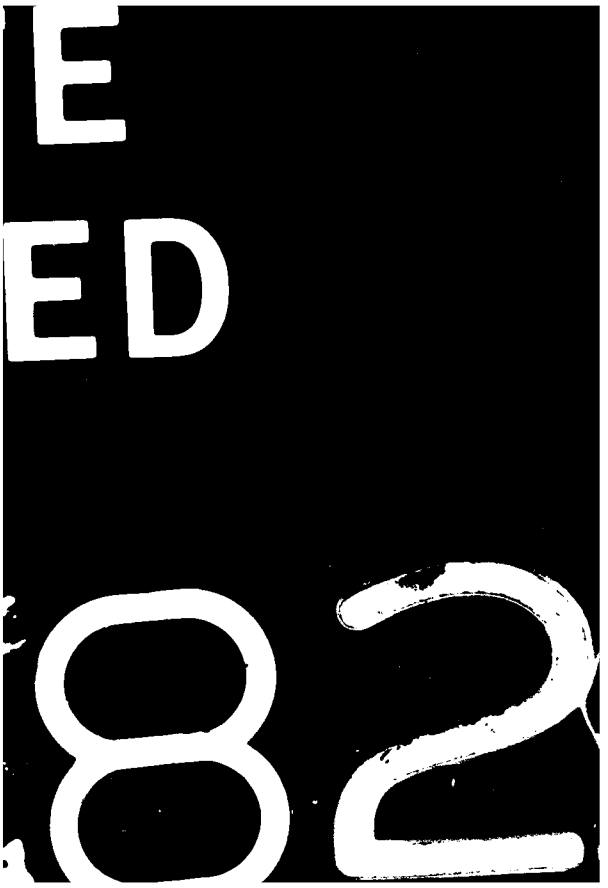
E
ED
82